

DISCOVERY OF PRECURSOR LBV OUTBURSTS IN TWO RECENT OPTICAL TRANSIENTS: THE FITFULLY VARIABLE MISSING LINKS UGC 2773-OT AND SN 2009ip

NATHAN SMITH^{1,2}, ADAM MILLER¹, WEIDONG LI¹, ALEXEI V. FILIPPENKO¹, JEFFREY M. SILVERMAN¹,
ANDREW W. HOWARD¹, PETER NUGENT³, GEOFFREY W. MARCY¹, JOSHUA S. BLOOM¹, ANDREA M. GHEZ⁴,
JESSICA LU⁴, SYLVANA YELDA⁴, REBECCA A. BERNSTEIN⁵, & JANET E. COLUCCI⁵

Draft version May 30, 2018

ABSTRACT

We present progenitor-star detections, light curves, and optical spectra of supernova (SN) 2009ip and the 2009 optical transient in UGC 2773 (U2773-OT), which were not genuine supernovae. Precursor variability in the decade before outburst indicates that both of the progenitor stars were luminous blue variables (LBVs). Their pre-outburst light curves resemble the S Doradus phases that preceded giant eruptions of the prototypical LBVs η Carinae and SN 1954J (V12 in NGC 2403), with intermediate progenitor luminosities. *Hubble Space Telescope* detections a decade before discovery indicate that the SN 2009ip and U2773-OT progenitors were supergiants with likely initial masses of 50–80 M_{\odot} and $\gtrsim 20 M_{\odot}$, respectively. Both outbursts had spectra befitting known LBVs, although in different physical states. SN 2009ip exhibited a hot LBV spectrum with characteristic speeds of 550 km s⁻¹, plus evidence for faster material up to 5000 km s⁻¹, resembling the slow Homunculus and fast blast wave of η Carinae. In contrast, U2773-OT shows a forest of narrow absorption and emission lines comparable to that of S Dor in its cool state, plus [Ca II] emission and an infrared excess indicative of dust, similar to SN 2008S and the 2008 optical transient in NGC 300 (N300-OT). The [Ca II] emission is probably tied to a dusty pre-outburst environment, and is not a distinguishing property of the outburst mechanism. The LBV nature of SN 2009ip and U2773-OT may provide a critical link between historical LBV eruptions, while U2773-OT may provide a link between LBVs and the unusual dust-obscured transients SN 2008S and N300-OT. Future searches will uncover more examples of precursor LBV variability of this kind, providing key clues that may help unravel the instability driving LBV eruptions in massive stars.

Subject headings: circumstellar matter — stars: evolution — stars: mass loss — stars: variables: other
— stars: winds, outflows — supernovae: general

arXiv:0909.4792v2 [astro-ph.SR] 31 Jan 2010

¹ Department of Astronomy, University of California, Berkeley, CA 94720-3411.

² email: nathans@astro.berkeley.edu.

³ Lawrence Berkeley National Laboratory, 1 Cyclotron Rd., Berkeley, CA 94720.

⁴ Division of Astronomy and Astrophysics, University of California, Los Angeles, CA 90095-1547.

⁵ Department of Astronomy and Astrophysics, 1156 High Street, UCO/Lick Observatory, University of California, Santa Cruz, CA 95064.

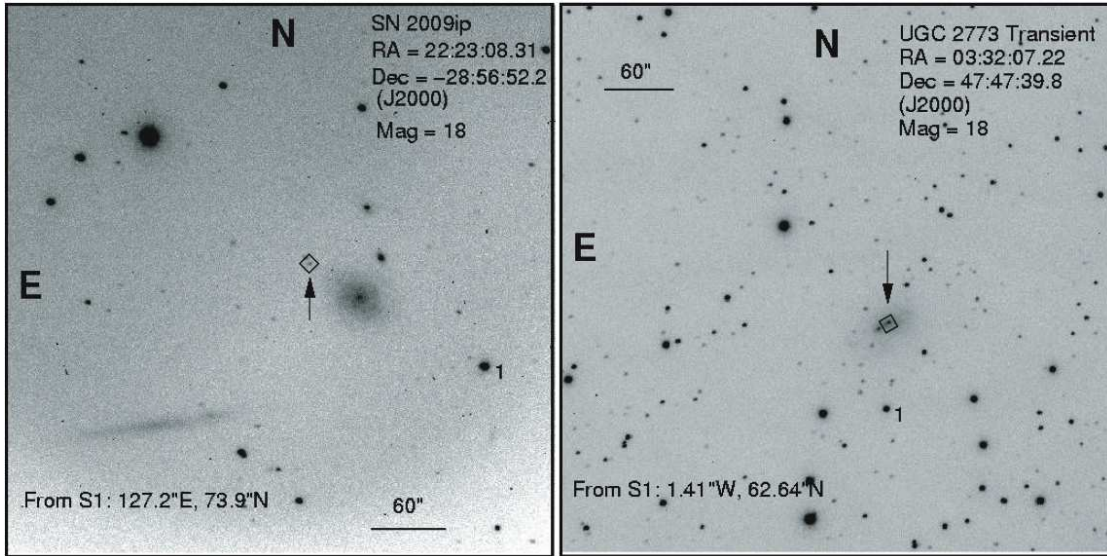


FIG. 1.— Finder charts showing the positions of SN 2009ip and U2773-OT with respect to their host galaxies. The small squares indicate the fields of view for the *HST*/WFPC2 F606W images in Figure 2. These are unfiltered images obtained with the Katzman Automatic Imaging Telescope (KAIT) at Lick Observatory.

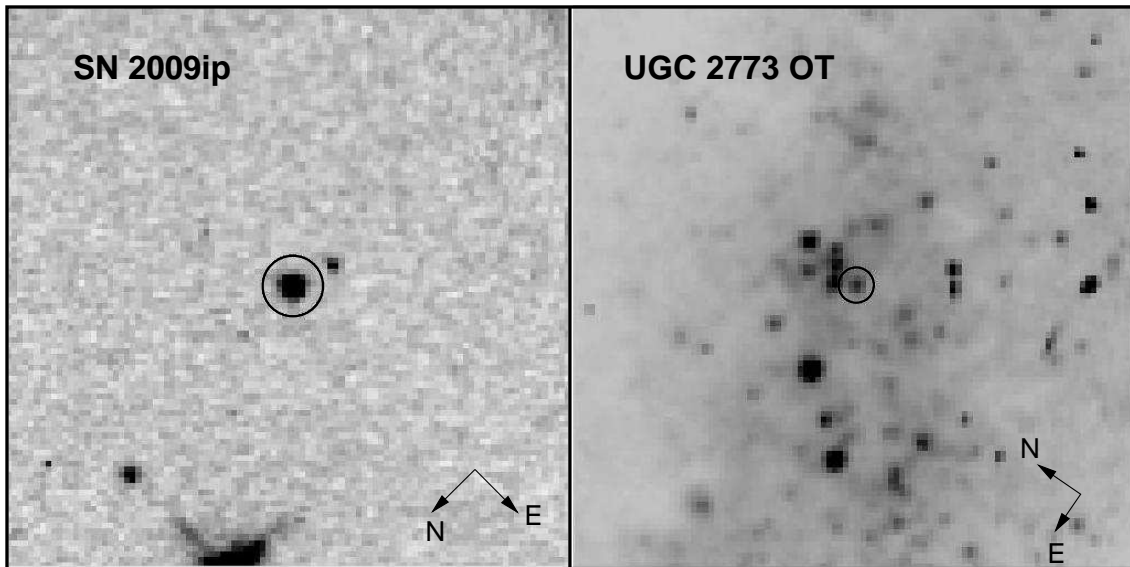


FIG. 2.— The sites of SN 2009ip and U2773-OT in the *HST*/WFPC2 F606W images. Each stamp is $10'' \times 10''$. The location of each transient as derived from high-resolution ground-based images is marked with a circle having a radius that is 15 times the 1σ uncertainty radius of the astrometric solution. A good candidate progenitor is identified for both transients.

1. INTRODUCTION

Among the objects discovered in the course of hunting for supernovae (SNe) are transient sources that are fainter and have slower expansion speeds than most core-collapse SNe. Following the historical examples (see Humphreys et al. 1999, and references therein) of the 19th century eruption of η Carinae, the 17th century eruption of P Cygni, SN 1954J (Variable 12 in NGC 2403), and SN 1961V, these transients have usually been associated with nonterminal eruptions of luminous blue variables (LBVs), rather than final explosions that mark the deaths of massive stars. LBVs represent a highly unstable, rapid mass-loss phase in the late evolution of massive stars (see Smith & Owocki 2006; Smith et al. 2004; Humphreys & Davidson 1994), which is still poorly understood. P Cygni and η Car remain as luminous well-studied blue supergiants, and the survivor of SN 1954J has been identified as a luminous dust-enshrouded star (Smith et al. 2001; Van Dyk et al. 2005). SN 1961V is a more controversial case (Chu et al. 2004), but there are indications of a surviving star as well (Goodrich et al. 1989; Filippenko et al. 1995; Van Dyk et al. 2002). Because the massive stars are thought to survive the events, recent examples of these η Car analogs such as SN 1997bs (Van Dyk et al. 2002) have earned the label “SN impostors.” For most recent extragalactic examples, however, available evidence that the star has survived remains inconclusive.

Interest in and interpretation of these transients was stirred by the surprising discovery that two recent events, SN 2008S and the 2008 optical transient in NGC 300 (hereafter N300-OT), both had relatively low-luminosity, dust-enshrouded progenitor stars (Prieto et al. 2008; Prieto 2008). Although the outburst properties resembled those of known LBV eruptions, interpretation of their dusty progenitors (Prieto et al. 2008; Thompson et al. 2009) implied initial masses below the usually recognized initial-mass range for LBVs extending down to $\sim 20 M_{\odot}$ (Smith et al. 2004). This fueled a range of speculation that these transients might be similar eruptive phenomena extending to somewhat lower mass and cooler stars (Smith et al. 2009; Berger et al. 2009a; Bond et al. 2009), the eruptive birth of a white dwarf and planetary nebula in stars with initial masses below $8 M_{\odot}$ (Thompson et al. 2009), electron-capture SNe (ecSNe) in extreme asymptotic giant branch (EAGB) stars around $8\text{--}10 M_{\odot}$ (Thompson et al. 2009; Botticella et al. 2009), faint core-collapse SNe (see Pastorello et al. 2007 in regard to previous events), or mergers/mass-transfer events related to some other recent transients (e.g., Kulkarni et al. 2007; Kashi et al. 2009). Interpretation of these objects remains controversial and puzzling.

Gogarten et al. (2009) found a likely initial mass of $12\text{--}25 M_{\odot}$ for the N300-OT progenitor based on the star-formation history of its local neighborhood, challenging the ecSN or white-dwarf birth hypotheses. Deriving a likely initial mass around $10\text{--}12 M_{\odot}$ from the luminosity (e.g., Prieto et al. 2008) depends upon the assumption that the progenitor was a cool EAGB star at the uppermost tip of its AGB. It remains possible, however, that the progenitors of SN 2008S and N300-OT were relatively blue stars that were heavily obscured by circumstellar dust (Prieto et al. 2008; Smith et al. 2009;

Berger et al. 2009a; Bond et al. 2009). In that case, the initial mass implied by the progenitor’s infrared (IR) luminosity would be closer to $15\text{--}20 M_{\odot}$ for N300-OT, and would therefore be in better agreement with the findings of Gogarten et al. (2009) than an $8\text{--}10 M_{\odot}$ EAGB star. The somewhat lower luminosity of the progenitor of SN 2008S would imply $12\text{--}15 M_{\odot}$ under the same assumption (Smith et al. 2009).

In this paper we discuss another pair of newly discovered transients with identified progenitors, the 2009 optical transient in UGC 2773 (hereafter U2773-OT) and SN 2009ip (see Fig. 1). U2773-OT occurred in the dwarf irregular galaxy UGC 2773, and was discovered (Boles 2009) on 2009 Aug. 18.08 (UT dates are used throughout this paper). SN 2009ip was discovered (Maza et al. 2009) on 2009 Aug. 26.11 in the Sb galaxy NGC 7259. Both objects had discovery absolute magnitudes fainter than -14 mag, and they had spectra with narrow H emission lines (Berger et al. 2009b; Berger & Foley 2009). These transient outbursts, still currently ongoing, share properties in common with giant LBV eruptions as well as SN 2008S and N300-OT. In these new cases, however, the progenitors are not as heavily obscured by dust. The progenitors are detected at optical wavelengths, and they exhibit pre-eruption variability that is matched by classic LBVs such as V12 and η Car. We reported the preliminary pre-outburst detections of SN 2009ip in Miller et al. (2009), while our photometry of U2773-OT is documented here for the first time. Based on their LBV-like pre-outburst variability, the two new transients help bridge the gap between classical LBV eruptions and objects similar to SN 2008S and N300-OT. Other than the historical cases of SN 1954J and SN 1961V, this is the first discovery of extended $5\text{--}10$ yr pre-eruption variability before an extragalactic LBV-like transient.

2. OBSERVATIONS

2.1. Pinpointing the Progenitors

Both SN 2009ip and U2773-OT had observations taken ~ 10 yr prior to discovery with the *Hubble Space Telescope*/Wide Field Planetary Camera 2 (*HST*/WFPC2), which we retrieved from the archive and analyzed. NGC 7259 (SN 2009ip) was observed in the F606W filter on 1999 Jun. 29, and UGC 2773 was observed in the F606W and F814W filters on 1999 Aug. 14.

To pinpoint the precise location of the two transients’ progenitors in the *HST* images, we obtained high-resolution ground-based images for comparison. On 2009 Sep. 9, we observed SN 2009ip in the K' band with the Near-Infrared Camera 2 (NIRC2) using the laser guide star (LGS) adaptive optics (AO) system (Wizinowich et al. 2006) on the 10-m Keck II telescope. Three mosaic pointings, each with three exposures of 4×15 s, were combined to yield a final stacked image with 9 min total exposure time, a pixel scale of $0''.04 \text{ pixel}^{-1}$, and a field of view of $41'' \times 41''$. For U2773-OT, we took a 20 s guider image with the high-resolution echelle spectrometer (HIRES; Vogt et al. 1994) on the 10-m Keck I telescope on 2009 Sep. 9. The image has a pixel scale of $0''.3 \text{ pixel}^{-1}$ and a field of view of $43'' \times 58''$.

To perform astrometric solutions between the ground-based and *HST* images, we adopted the technique detailed by Li et al. (2007) using stars present in both the

TABLE 1
PHOTOMETRY OF SN 2009IP

MJD	filter	mag	1σ	data source
51358.50	F606W	21.8	0.2	HST
53195.47	<i>R</i>	>21.17	...	DS
53226.33	<i>R</i>	>21.43	...	DS
53233.25	<i>R</i>	>20.97	...	DS
53251.23	<i>R</i>	>21.01	...	DS
53259.21	<i>R</i>	>20.65	...	DS
53541.44	<i>R</i>	20.61	0.14	DS
53554.46	<i>R</i>	20.37	0.16	DS
54305.39	<i>R</i>	20.97	0.22	DS
54323.35	<i>R</i>	20.92	0.25	DS
54701.33	<i>R</i>	>21.51	...	DS
54702.33	<i>R</i>	>21.33	...	DS
55043.50	unfiltered	18.5	0.4	CBET 1928
55069.61	unfiltered	17.9	0.3	CBET 1928
55071.75	unfiltered	17.0	0.3	CBET 1928
55073.50	<i>R</i>	18.2	0.1	KAIT
55085.10	unfiltered	20.2	0.2	guider
55096.50	unfiltered	18.3	0.2	guider
55097.50	<i>R</i>	18.3	0.2	KAIT

ground-based and *HST* images. Due to the small field of view of the ground-based images, we are only able to measure the positions for five stars in each field. The astrometric solutions using IRAF/GEOMAP yield a precision of 36 mas and 21 mas for SN 2009ip and U2773-OT, respectively⁶. The positions of the transients are then mapped onto the *HST* images. Due to the small available number of stars, we only use second-order polynomials in the astrometric transformations. We also conducted an additional error analysis by taking out one star and leaving four with which to perform the solution, and repeating this for all stars. For both transients, the average position from the five separate measurements and the associated uncertainty is fully consistent with the position measured from the solution using all five stars together, so our solutions appear to be stable despite the small number of stars involved.

Figure 2 shows a $10'' \times 10''$ region of the sites for the transients in the *HST*/WFPC2 images. A candidate progenitor is detected for both transients within 1σ precision of the astrometric solution. We therefore confirm the candidate progenitors marked in Figure 2, first proposed for SN 2009ip by our group (Miller et al. 2009) and for U2773-OT by Berger & Foley (2009). The *HST* photometry for the progenitors is measured with HSTphot (Dolphin 2000a, 2000b) and listed in Tables 1 and 2. HSTphot also reports that both objects have a stellar point-spread function (PSF): they belong to type “1” (good star), with a sharpness well within the range of ± 0.3 as suggested by Leonard et al. (2008). The coordinates of the two transients, as measured directly from the World Coordinate System (WCS) in the WFPC2 FITS images, are $\alpha_{J2000} = 3^{\text{h}}32^{\text{m}}07^{\text{s}}.22$, $\delta_{J2000} = 47^{\circ}47'39''.4$ for U2773-OT and $\alpha_{J2000} = 22^{\text{h}}23^{\text{m}}08^{\text{s}}.20$, $\delta_{J2000} = -28^{\circ}56'52''.6$ for SN 2009ip.

2.2. Pre-Eruption Photometry

In Figure 3 we plot absolute magnitudes derived from the photometry listed in Tables 1 and 2. For SN 2009ip

⁶ Although the ground-based AO image of SN 2009ip has much higher resolution than the U2773-OT image, the astrometric solution is less precise because of the faintness of stars in the image.

TABLE 2
PHOTOMETRY OF U2773-OT

MJD	filter	mag	1σ	data source
51404.1	F606W	22.83	0.03	HST
51404.1	F814W	22.22	0.05	HST
51853.5	unfiltered	>20.80	...	KAIT (stack)
52225.5	unfiltered	>21.10	...	KAIT (stack)
52589.5	unfiltered	>21.00	...	KAIT (stack)
52939.5	unfiltered	>20.60	...	KAIT (stack)
53683.0	unfiltered	19.91	0.42	KAIT (stack)
54042.5	unfiltered	19.16	0.07	KAIT (stack)
54394.9	unfiltered	18.93	0.10	KAIT (stack)
54772.1	unfiltered	18.73	0.06	KAIT (stack)
55051.5	unfiltered	17.96	0.10	KAIT
55061.5	unfiltered	17.70	0.19	KAIT
55072.5	unfiltered	17.91	0.06	KAIT
55077.5	unfiltered	17.76	0.05	KAIT
55079.5	unfiltered	17.76	0.03	KAIT
55081.5	unfiltered	17.82	0.04	KAIT
55082.5	unfiltered	17.76	0.03	KAIT
55083.5	unfiltered	17.79	0.03	KAIT
55084.5	unfiltered	17.61	0.12	KAIT
55090.5	unfiltered	17.74	0.03	KAIT
55091.5	unfiltered	17.73	0.03	KAIT
55092.5	unfiltered	17.75	0.03	KAIT
55094.5	unfiltered	17.75	0.03	KAIT
55095.5	unfiltered	17.72	0.03	KAIT
55096.5	unfiltered	17.68	0.03	KAIT
55097.5	unfiltered	17.71	0.03	KAIT
55098.5	unfiltered	17.67	0.03	KAIT
55099.5	unfiltered	17.67	0.03	KAIT
55100.5	unfiltered	17.74	0.03	KAIT
55102.5	unfiltered	17.71	0.03	KAIT
55105.5	unfiltered	17.67	0.04	KAIT
55110.5	unfiltered	17.69	0.05	KAIT
55113.5	unfiltered	17.71	0.03	KAIT
55120.5	unfiltered	17.65	0.03	KAIT
55123.5	unfiltered	17.59	0.03	KAIT
55126.5	unfiltered	17.62	0.03	KAIT
55129.5	unfiltered	17.57	0.03	KAIT
55132.5	unfiltered	17.55	0.03	KAIT
55133.5	unfiltered	17.57	0.03	KAIT
55136.5	unfiltered	17.67	0.04	KAIT
55149.5	unfiltered	17.52	0.03	KAIT
55152.5	unfiltered	17.57	0.03	KAIT
55155.5	unfiltered	17.65	0.03	KAIT
55158.5	unfiltered	17.60	0.03	KAIT
55161.5	unfiltered	17.72	0.03	KAIT
55164.5	unfiltered	17.56	0.03	KAIT
55169.5	unfiltered	17.66	0.03	KAIT
55173.5	unfiltered	17.60	0.05	KAIT

TABLE 3
PAIRITEL PHOTOMETRY OF U2773-OT

MJD	<i>J</i> (mag)	<i>H</i> (mag)	<i>K</i> (mag)
55082.50	15.57±0.09	14.64±0.15	14.97±0.25
55090.36	15.99±0.13	15.07±0.12	15.19±0.16
55091.40	15.89±0.15	14.95±0.16	14.87±0.19
55092.36	15.99±0.16	15.13±0.15	15.1±0.2
55095.35	15.82±0.14	14.84±0.09	14.88±0.24
55096.41	15.97±0.13	15.06±0.11	14.94±0.23
55099.42	15.85±0.17	14.93±0.12	14.98±0.14
55102.43	15.87±0.13	14.89±0.14	14.99±0.09
55113.41	15.96±0.21	15.04±0.18	14.91±0.17
55119.41	15.69±0.14	14.84±0.15	14.78±0.18
55122.43	15.8±0.14	14.84±0.11	14.8±0.19
55125.43	15.75±0.12	15.18±0.15	15.11±0.18
55180.13	15.55±0.1	14.71±0.13	14.68±0.14
55182.07	15.47±0.12	14.79±0.11	14.61±0.13

TABLE 4
 SPECTROSCOPIC OBSERVATIONS

Date	Tel./Inst.	Target	day	Exp. (s)	$\lambda(\text{\AA})$	comment
2009 Sep. 10	Keck/HIRES	U2773-OT	22	1800	6543-7990	only red lines detected
2009 Sep. 11	Keck/HIRES	SN 2009ip	16	1200	6543-7990	only $H\alpha$ detected
2009 Sep. 21	Keck/LRIS	U2773-OT	34	300	3800-5100	med. resolution
2009 Sep. 21	Keck/LRIS	U2773-OT	34	300	6250-7850	med. resolution
2009 Sep. 21	Keck/LRIS	U2773-OT	34	300	3600-9200	low resolution
2009 Sep. 21	Keck/LRIS	SN 2009ip	25	780	3800-5100	med. resolution
2009 Sep. 21	Keck/LRIS	SN 2009ip	25	640	6250-7850	med. resolution
2009 Sep. 21	Keck/LRIS	SN 2009ip	25	300	3600-9200	low resolution

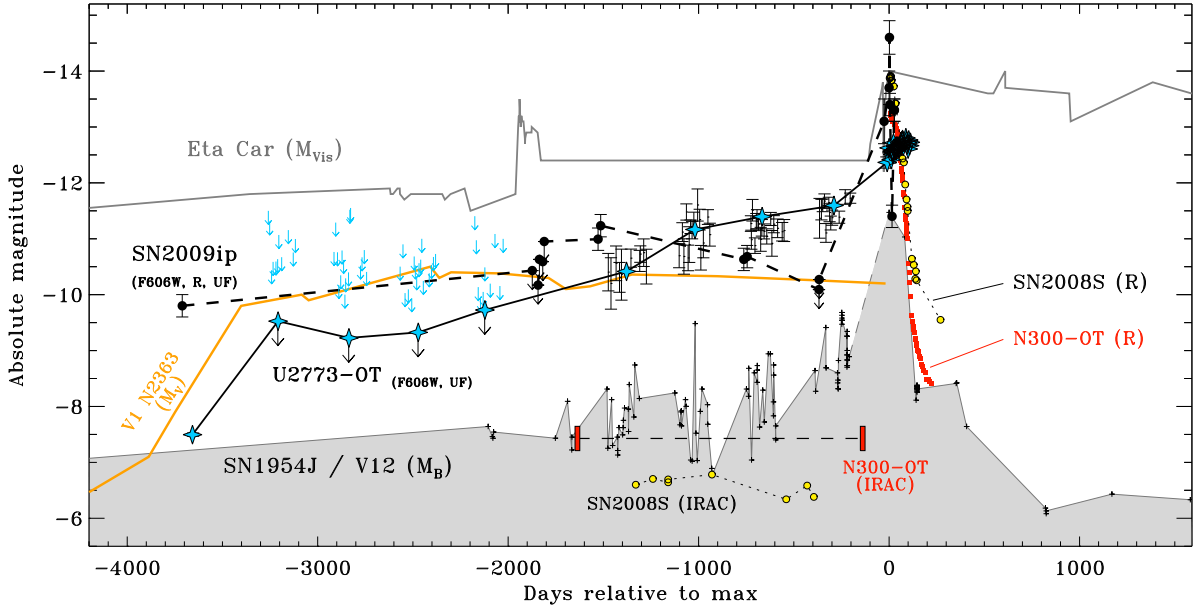


FIG. 3.— Our absolute-magnitude light curves of the LBV-like transients SN 2009ip and U2773-OT (Tables 1 and 2) compared to the historical LBVs η Carinae in its 19th century “Great Eruption” (compiled by Frew 2004) and SN 1954J (V12 in NGC 2403; Tammann & Sandage 1968). The orange curve is the LBV eruption of V1 in NGC 2363 (Drissen et al. 2001; Petit et al. 2006), although shifted to an arbitrary date. We also include R -band light curves of the recent transients N300-OT (from Bond et al. 2009) and SN 2008S (from Smith et al. 2009), along with their pre-outburst bolometric magnitudes derived from *Spitzer*/IRAC data (Prieto et al. 2008; Prieto et al. 2009; Bond et al. 2009). For U2773-OT, we show both upper limits or detections from individual exposures (arrows and error bars, respectively), as well as upper limits and detections in stacked seasonal data (blue stars). The earliest detections of both objects were from archival *HST* F606W data, corrected appropriately for Galactic extinction.

in NGC 7259, we adopt a distance modulus of $m - M = 31.55$ mag, and a Galactic reddening and extinction of $E(B - V) = 0.019$ mag and $A_R = 0.05$ mag, respectively. Similarly, for U2773-OT we adopt $m - M = 28.82$ mag, $E(B - V) = 0.56$ mag, and $A_R = 1.51$ mag. The observations are described below. The light curves are also shown in Figure 4, which focuses on the time around peak luminosity.

The field of SN 2009ip was imaged multiple times during the operations of the Palomar-Quest survey, and those observations have been reprocessed as part of the DeepSky project⁷ (DS; Nugent 2009). As first noted by Miller et al. (2009), a source at the location of SN 2009ip was observed in 2005, 4 yr prior to discovery, and it was at comparable luminosity in 2007. DS typically has more than one image on any given night when a field was observed, so we stack all DS images taken on the same night to improve the limiting magnitude for each epoch. Deep Sky images were obtained through a nonstandard red

filter that has a blue cutoff at $\lambda \approx 6100$ \AA , and are otherwise similar to unfiltered photometry, which we take to be comparable to R -band (see below). DS photometry of SN 2009ip was calibrated relative to the USNO-B1.0 red magnitudes, with typical uncertainties of 0.1–0.2 mag when several USNO stars are used.

The full historical DS light curve of SN 2009ip is shown in Figure 3, while the photometry is reported in Table 1. Figures 3 and 4 also include data around the time of discovery (Maza et al. 2009) and our own R -band photometry obtained with the 0.76-m Katzman Automatic Imaging Telescope (KAIT; Filippenko et al. 2001; Filippenko 2003) at Lick Observatory (see below). The KAIT R -band photometry is calibrated relative to the USNO-B1.0 red magnitudes. It is unclear how the unfiltered discovery magnitudes reported by Maza et al. (2009) are calibrated, so we give large uncertainties for these particular measurements. Moreover, as discussed by Li et al. (2003), unfiltered data are often clearly matched to the broad R band. A source at the position of SN 2009ip is seen in the *HST*/WFPC2 image taken ~ 10 yr before dis-

⁷ <http://supernova.lbl.gov/~nugent/deepsky.html>.

covery, with $m_{F606W} = 21.8 \pm 0.2$ mag. At the distance of NGC 7259 this implies $M_V \approx -9.8$ mag. The early *HST* detection, if this is the quiescent progenitor star, thus requires a high luminosity of at least $\log(L/L_\odot) \approx 5.9$ (higher for a nonzero bolometric correction), and implies a high initial mass of 50–80 M_\odot (e.g., Lejeune & Schaerer 2001).

UGC 2773, the dwarf irregular host galaxy of U2773-OT, is monitored regularly with KAIT. We analyzed pre-discovery unfiltered (approximately *R* band) images and detected a source at the position of U2773-OT during the ~ 5 yr before discovery, as well as upper limits before that. There were multiple observations each year, so we produced stacked seasonal averages to improve the sensitivity. A stacked image from the year 2000, when U2773-OT was not detected, is used as a template image in an image-subtraction technique to cleanly remove the galaxy contamination at the position of U2773-OT in later images. The resulting upper limits and detections are listed in Table 2, while these averaged data as well as individual epochs are shown in Figure 3.

As noted above, U2773-OT was also detected in archival *HST*/WFPC2 images about 10 yr before discovery, and these *HST* magnitudes are listed in Table 2 as well. F606W is not a standard *V*-band filter, so we used SYNPHOT to convert it in order to interpret the F606W–F814W color. Using SYNPHOT and adopting the Galactic reddening of $E(B - V) = 0.564$ mag along the line of sight to U2773, the object has $M_V \approx -7.8$ mag, and an intrinsic $V - I$ color of ~ 0.09 mag, or less if there was additional circumstellar reddening as we strongly suspect (see below). This corresponds to an early A-type supergiant or hotter, with $\log(L/L_\odot) \geq 5.1$, and an initial mass of at least 20 M_\odot . This is much like the LBV star HD 168625 (Smith 2007), and it has the same spectral type but is less luminous than the yellow hypergiant IRC+10420 which, interestingly, has a spectrum similar to that of the U2773-OT outburst, as we discuss below. We find it quite likely, however, that the progenitor star had some additional circumstellar dust based on its IR excess (§3.5), in which case it was even hotter, more luminous, and more massive than our estimates from *HST* data alone.

2.3. Infrared Photometry During Eruption

We observed U2773-OT simultaneously in the *JHK_s* bands with the 1.3-m Peters Automated Infrared Imaging Telescope (PAIRITEL; Bloom et al. 2006), beginning on 2009 Sep. 8 (day 21 after discovery) and at several subsequent epochs as listed in Table 3. The PAIRITEL observations were scheduled and obtained automatically by the robotic telescope, and the images were processed and reduced as part of an automatic pipeline. Archival Two Micron All Sky Survey (2MASS; Skrutskie et al. 2006) images of the field taken on 1998 Nov. 11 were used as reference data for image differencing. We performed PAIRITEL–2MASS image subtraction using HOTPANTS⁸, and measured the flux of the transient in the difference images via aperture photometry. The photometry was calibrated relative to the 2MASS stars in the field. To estimate the uncertainties we inserted fake stars at the measured magnitude of U2773-OT on top of

locations in the host galaxy that had a surface brightness similar to that of the transient’s location. We subtracted the 2MASS image from the images with fake stars, and measured the scatter in the fake-star flux to determine the uncertainty in the flux of the transient. The final *JHK_s* photometry is listed in Table 3 and is plotted in Figure 5. During the time of our observations, the near-IR flux from U2773-OT has shown a slight increase over ~ 100 days, commensurate with the slow brightening in optical photometry, and with relatively constant color.

Using the stacked *K'* image of SN 2009ip (§2.1), we attempted to measure its *K'* magnitude. In a deep PAIRITEL image, in which we do not detect SN 2009ip, we do detect a star located at $\alpha_{J2000} = 22^{\text{h}}23^{\text{m}}08^{\text{s}}.503$, $\delta_{J2000} = -28^\circ 56' 47''.75$, which is common to both the PAIRITEL and AO images. Calibrating relative to 2MASS we measure $K_s = 15.93 \pm 0.12$ mag for this star. Assuming $K_s \approx K'$ (the *K'* and *K_s* filters are approximately the same), we therefore measure $K' = 19.68 \pm 0.12$ mag for SN 2009ip on 2009 Sep. 9.

2.4. Spectroscopy

A summary of our spectroscopic observations is listed in Table 4. We obtained high-resolution ($R = \lambda/\Delta\lambda \approx 60,000$) optical echelle spectra of U2773-OT on 2009 Sep. 10 using HIRES (Vogt et al. 2004) on the 10-m Keck I telescope. The HIRES spectra were reduced using standard procedures. These observations correspond to day 22 after discovery for U2773-OT. We used the B5 decker (0''.86 slit width) and a total exposure time of 1800 s. The instrument covers the wavelength range 3642–7990 Å, but with gaps in the wavelength coverage because the spectrum is dispersed onto three different detectors; because of the low signal-to-noise ratio (S/N), we only used data on the red chip over the interval 6543–7990 Å. This was a single exposure, so individual cosmic rays in the extracted spectrum were masked out; these features were always a few pixels wide and did not significantly impact the line profiles.

The spectrum has very low S/N in the blue range, but several emission lines are detected at red wavelengths. The spectrum reveals narrow emission lines of H α , [N II] $\lambda\lambda 6548, 6583$, and [S II] $\lambda\lambda 6716, 6731$ having full width at half-maximum intensity (FWHM) $\approx 49 \text{ km s}^{-1}$ (much wider than the instrument resolution of $\sim 5 \text{ km s}^{-1}$); these are due to an underlying H II region that was not subtracted, or perhaps an extended circumstellar nebula. In addition, H α has a broader base attributable to the transient. The HIRES spectrum of U2773-OT in the wavelength range around H α is shown in Figure 6. The underlying broad feature has a clear P Cygni profile, which can be fit with a combination of an emission line having Gaussian FWHM $\approx 360 \text{ km s}^{-1}$ and another Gaussian in absorption. The P Cygni absorption trough is at -350 km s^{-1} , in agreement with velocities quoted by Berger & Foley (2009) in an earlier spectrum.

We obtained a HIRES spectrum of SN 2009ip on the following night, 2009 Sep. 11 (day 16). Despite good conditions, the 20-min exposure was not deep enough to detect the continuum, and subsequent analysis of unfiltered photometry of the guider image revealed that SN 2009ip had faded more than we anticipated, to 20.2 mag. Our HIRES observation was conducted at or near the mini-

⁸ <http://www.astro.washington.edu/users/becker/hotpants.html>.

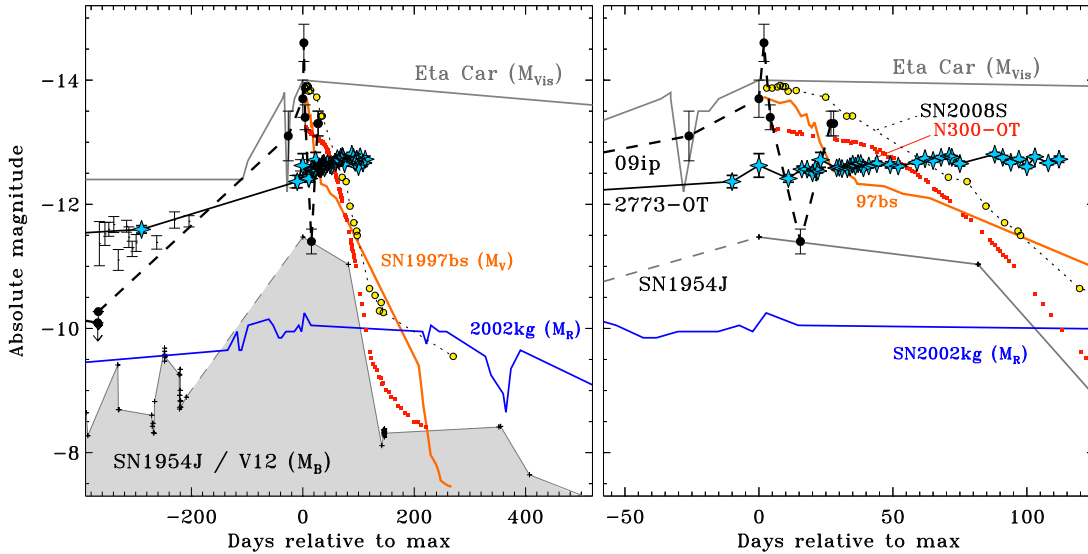


FIG. 4.— Same as Figure 3, but zooming in on the time period near maximum light. Plotting symbols for SN 2009ip, U2773-OT, SN 2008S, and N300-OT are the same as in Figure 3. For comparison at this scale, we have also added the V -band light curve of SN 1997bs (orange; Van Dyk et al. 2000) and the unfiltered/ R -band light curve of SN 2002kg (blue; Van Dyk et al. 2006). The right panel shows an expanded view of the left panel.

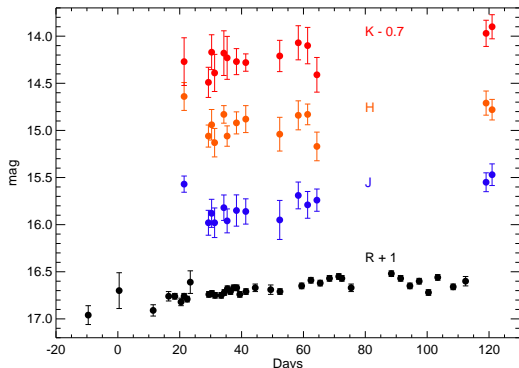


FIG. 5.— The near-IR apparent JHK_s photometry of U2773-OT in days after discovery (2009 Aug. 18.08) obtained with PAIRITEL, compared to the KAIT unfiltered ($\sim R$ -band) optical photometry.

imum of a sudden fading episode, discussed at length in §3.2. At this epoch, however, we did detect the $H\alpha$ emission line, which has a total line flux of 0.7×10^{-14} erg s^{-1} cm^{-2} (this is one third the value measured in lower-resolution spectra obtained a few days later; see below). The HIRES $H\alpha$ line profile in SN 2009ip is shown in Figure 7; the spectrum is very noisy, even though the pixels have been binned by a factor of 4. Given the quality of the data, the line can be approximated adequately by a Lorentzian profile with $FWHM \approx 550$ km s^{-1} ; this is the same profile that is well fit to the lower-resolution spectrum (see below). We do not clearly detect any narrow component from an underlying H II region around SN 2009ip, although this is not necessarily surprising as many nearby LBVs are not in bright H II regions.

Later, on 2009 Sep. 21, we observed SN 2009ip again, this time with the Low Resolution Imaging Spectrometer (LRIS; Oke et al. 1995) on Keck I. To our surprise, unfiltered photometry in the guider image revealed that SN 2009ip had rebrightened to 18.3 mag (listed in Table 1), returning almost to its peak brightness. The conditions were photometric, with $0''.85$ seeing, so we obtained

spectra of both SN 2009ip and U2773-OT. We observed with the same LRIS setup for both SN 2009ip and U2773-OT, consisting of medium-resolution ($0''.7$ slit width; 1200 lines mm^{-1} grating; 3 \AA pixel $^{-1}$) and low-resolution ($1''.0$ slit width; 400 lines mm^{-1} grating; $\sim 6 \text{ \AA}$ pixel $^{-1}$) red-side settings. On the blue side, a 400 lines mm^{-1} grism was used in both settings, providing spectra with $\sim 3 \text{ \AA}$ pixel $^{-1}$. The medium-resolution setting yielded blue and red spectra in the wavelength ranges 3120 – 5594 \AA and 6250 – 7880 \AA , respectively, while the low-resolution setting covered the full range 3246 – $10,260 \text{ \AA}$ (the bluest wavelengths were clipped due to noise). For SN 2009ip, we used exposure times of 780 s (blue side, medium resolution), 2×320 s (red side, medium resolution), and 300 s (both sides, low resolution). For U2773-OT, all exposures were 300 s.

The reduction of the U2773-OT spectrum was complicated because the long-slit spectra revealed extended emission along the slit due to a background H II region or extended circumstellar nebula within a few tenths of an arcsecond from the transient. This background H II region emission was sampled on either side of the source and carefully subtracted from the spectrum, although some subtraction residuals remained at low levels (see, for example, the [S II] lines in the red-side spectrum).

Figures 8 and 9 show the final medium-resolution LRIS spectra of both transients in the blue and red, respectively, while Figure 10 zooms in on the $H\alpha$ profiles of each. Figure 11 displays the wavelength range around the red [Ca II] lines seen in the LRIS spectra for both targets, as well as the HIRES data for U2773-OT. Figure 12 shows the wavelength range around Na I D and He I $\lambda 5876$ in the low-resolution LRIS spectra, which is in a spectral region excluded by the medium-resolution LRIS data. Finally, the full low-resolution LRIS spectra of both SN 2009ip and U2773-OT are shown in Figure 13. In Figure 13 we compare these low-resolution LRIS spectra of both transients to spectra of the yellow hypergiant IRC+10420 (from Smith et al. 2009), as well as SN 2008S

(Smith et al. 2009) and the LBV SN 1997bs (Van Dyk et al. 2002) during eruption. The low-resolution LRIS spectrum of U2773-OT was qualitatively similar, although superior to, a spectrum obtained at Lick Observatory three nights earlier, which is not shown here.

3. RESULTS

3.1. Light-Curve Comparison

Absolute-magnitude light curves for SN 2009ip and U2773-OT are displayed in Figure 3, where they are compared with those of several other objects. The gray line shows the historical visual light curve of η Car during its 19th century “Great Eruption,” compiled from historical sources by Frew (2004). It showed gradual brightening 10 yr before peak, a pre-outburst event in 1837, and then finally the $M_{\text{Visual}} \approx -14$ mag peak of its eruption in 1843, followed by a slow and irregular decline over the next decade. While η Car is the most famous and best studied LBV, it is certainly not representative of all LBVs. The prolonged eruption, in particular, is highly unusual.

We also show the B -band light curve of the prototypical LBV eruption SN 1954J (V12 in NGC 2403; shaded gray in Figure 3) from Tammann & Sandage (1968), corrected for Galactic extinction. Before the LBV eruption began, the quiescent star was considerably less luminous than η Car, with an absolute B magnitude of only about -7 to -7.5 mag. Yet, Tammann & Sandage (1968) noted that it was a key example of the class of bright blue irregular variables like those in M31 and M33 (Hubble & Sandage 1953), later termed “LBVs,” and the star is now known to have survived the event (Smith et al. 2001; Van Dyk et al. 2005). The progenitor, V12, is a member of the less luminous class of LBVs with initial masses of 20–40 M_{\odot} (Smith et al. 2004). V12 showed rapid irregular variability in the ~ 5 yr leading up to its outburst, with oscillations of 1–2 mag. (This “flickering” is discussed more in §3.2 below.) Such rapid variability is unusual, but V12 also has unusually well-sampled pre-eruption photometry. The cause of these wild oscillations is unknown, but they probably signify a growing instability in the star and herald the approaching runaway of the SN 1954J event itself.⁹

Another case to consider is the more recent and well-studied LBV outburst V1 in the nearby dwarf irregular galaxy NGC 2363. The absolute V light curve from Drissen et al. (1997, 2001; see also Petit et al. 2006) is shown with the orange curve in Figure 3. (Its dwarf host with metallicity similar to that of the Small Magellanic Cloud is particularly relevant for U2773-OT.) V1 is noteworthy because, again, its LBV eruption came from a star whose initial luminosity was low compared to that of η Car — in fact, its quiescent pre-outburst luminosity was equivalent to the IR luminosity of SN 2008S, also shown in Figure 3 (more details are given below). During its decade-long outburst in the 1990s, its M_V brightened by ~ 3.5 mag and remained so for several years. Unlike the historical examples of V12 and η Car, V1 has

been subject to detailed non-LTE (local thermodynamic equilibrium) modeling of its outburst spectrum, revealing $\log(L/L_{\odot}) \approx 10^{6.4}$ and $R/R_{\odot} \approx 300$ –400 during its outburst, and a strong stellar wind with $v_{\infty} \approx 300$ km s^{-1} (Drissen et al. 2001). The radius of the photosphere, however, only increased at a rate of ~ 4 km s^{-1} (i.e., much slower than the steady wind expansion), so this was not an explosion. V1 lives within the well-known “mini-starburst” giant H II region NGC 2366 (Drissen et al. 1997) in the galaxy NGC 2363, surrounded by many young, massive stars. This is a well-established case of a super-Eddington wind outburst from a massive star, despite the apparently low luminosity of its quiescent-phase progenitor. The LBV outburst of V1 is similar in duration and absolute magnitude to the precursor outbursts of the two new transients presented in this paper, although the V1 LBV outburst has not (as yet) culminated in a comparably bright giant eruption phase with $M_V \lesssim -12$ mag; instead, it appears to be an example of a fainter and prolonged LBV eruption.

Both SN 2009ip and U2773-OT stand in between η Car and SN 1954J, with all four objects showing precursor variability in the decade leading up to the peak of their giant eruptions. Again, the cause for this is not known, but the phenomenon is a well-established property of some LBVs (e.g., Humphreys et al. 1999). This precursor variability and the range of luminosity of the progenitors makes a strong case that SN 2009ip and U2773-OT are, in fact, both *bona fide* giant LBV eruptions from massive stars that were in a prolonged outburst phase before their discovery.

Figure 3 also includes some available information for SN 2008S and N300-OT, and their dust-obscured progenitors. The light curves of their eruptions show peak absolute magnitudes of roughly -14 mag, with a relatively fast decline over 100–200 days resembling that of SN 1954J. Their similarity to LBV eruptions was already noted in previous papers (Smith et al. 2009; Berger et al. 2009a; Bond et al. 2009; Prieto et al. 2008; Thompson et al. 2009), but they were surprising because of their relatively low-luminosity progenitors compared to LBVs. However, Figure 3 shows that *their progenitor luminosities are not that low after all*. The plotted quantities in Figure 3 are the bolometric luminosities derived from fits to the mid-IR spectral energy distributions (SEDs) measured in *Spitzer* data (Prieto et al. 2008; Prieto 2008; Bond et al. 2009). While their luminosities may overlap with the most extreme AGB stars at the very tip of their evolution (Thompson et al. 2009), the luminosity of N300-OT is the same as the pre-outburst luminosity of V12 in NGC 2403, known to be an LBV, and is very close to the pre-outburst luminosity of U2773-OT. The IR luminosity of the SN 2008S progenitor is only a factor of ~ 2 less, and is comparable to the quiescent luminosity of the LBV V1 in NGC 2363. This makes it plausible that both of these transients were moderately massive stars, comparable to or somewhat less massive than V12. This LBV connection is reinforced by a spectral comparison, discussed later.

An obvious caveat is that we are comparing integrated IR luminosities of dust-enshrouded progenitors (for SN 2008S and N300-OT) to estimates of the luminosity based on visual-wavelength photometry. The

⁹ While the peak of the SN 1954J eruption was fainter than others in Figure 3, it is worth noting that it was not observed for ~ 7 months before peak, and Tammann & Sandage (1968) suspected that a brighter peak magnitude may have occurred during that hiatus from observing. We indicate this time interval with a dashed line in Figs. 3 and 4.

comparison in Figure 3 assumes bolometric corrections of zero for the optically identified sources, and does not include possible IR excesses or correction for local extinction, so these luminosities are actually lower limits. However, the integrated mid-IR luminosities of SN 2008S and N300-OT are also lower limits, since they only represent the luminosity absorbed and reradiated by warm dust, whereas radiation may escape in other directions that we cannot see without heating dust if the dust shells are nonspherical (in the case of an edge-on dust torus, for example). In any case, further corrections beyond the values shown in Figure 3 become very uncertain, but could only raise the luminosities shown here.

3.2. Peak Luminosity, Decline Rates, and “Flickering”

The photometric behavior around the time of peak luminosity is unusual for both transients. Figure 4 shows the same light curves as in Figure 3, but on an expanded scale to illustrate the details of the giant eruptions themselves.

In the 5 yr before discovery, U2773-OT was apparently in an unstable pre-outburst state. It continually rose in brightness, culminating in its peak absolute R magnitude of about -12.8 . The total increase was $\Delta m \approx 5$ mag. It has remained roughly at that luminosity for a few months afterward, showing minor oscillations with amplitudes of no more than 0.2 mag on timescales of several days.

SN 2009ip was different and rather astonishing. After its precursor eruption ~ 5 yr before discovery, it settled to a fainter state, with only upper limits of about -10 mag at ~ 1 yr before discovery. This may mark a temporary return to its quiescent state seen by *HST*. It then brightened to $M_R = -13$ mag, and continued to rise to a peak magnitude even brighter than that of η Car, at $M_R = -14.5$ mag. The total increase in brightness from its pre-outburst state was ~ 4.7 mag. Unexpectedly, however, SN 2009ip suddenly faded by 3.2 mag in ~ 16 days, only to recover again soon after (Fig. 4). We announced our discovery of this startling dip and recovery shortly before submitting this paper (Li et al. 2009).

In connection with the transients SN 2008S and N300-OT, one may wonder if their fast decline rates are consistent with LBVs. In fact, several well-studied LBVs have shown extremely fast decline rates. At ~ 100 days after peak, V12/SN 1954J exhibited a very rapid decline rate of 0.05 mag day^{-1} , comparable to those of SN 2008S and N300-OT (Fig. 4). SN 1997bs also showed an extremely rapid 1.5 mag decline from its peak magnitude in the first 20 days, although that decline rate varied later. Even η Car had a rapid rise and decline associated with its events in 1837 and 1843 (Fig. 3).

In this context, the astonishingly fast decline of SN 2009ip from its maximum luminosity is quite important. Its prediscovery luminosity and variability establish that it is a true LBV, yet it fades faster than any of the historical LBVs, SN impostors, or the controversial transients SN 2008S and N300-OT. The sharp fading and rebrightening of SN 2009ip is even more extreme than the fluctuations experienced by η Car in 1837 and 1843, providing some assurances that the rapid 19th century fluctuations observed by J. F. W. Herschel may have, in fact, been real, leading him (see Herschel 1847) to describe η Car as “a star fitfully variable to an astonishing extent... apparently with no settled period and no regu-

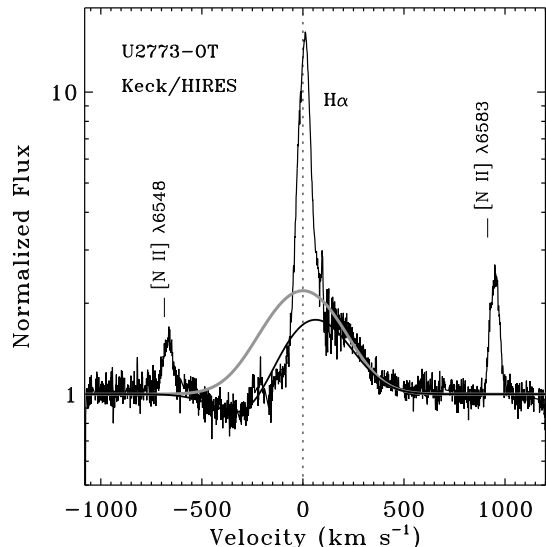


FIG. 6.— HIRES spectrum of U2773-OT on day 22, showing $H\alpha$ and the narrow $[N\ II]$ lines. The thick gray curve is a Gaussian with $\text{FWHM} = 360$ km s^{-1} , and the thin black curve is the same Gaussian with a blueshifted P Cygni absorption component subtracted. The absorption minimum is at -350 km s^{-1} . The narrow components of all lines have Gaussian $\text{FWHM} \approx 49$ km s^{-1} , and arise in an underlying $H\ II$ region or extended circumstellar nebula that was not subtracted from the HIRES data.

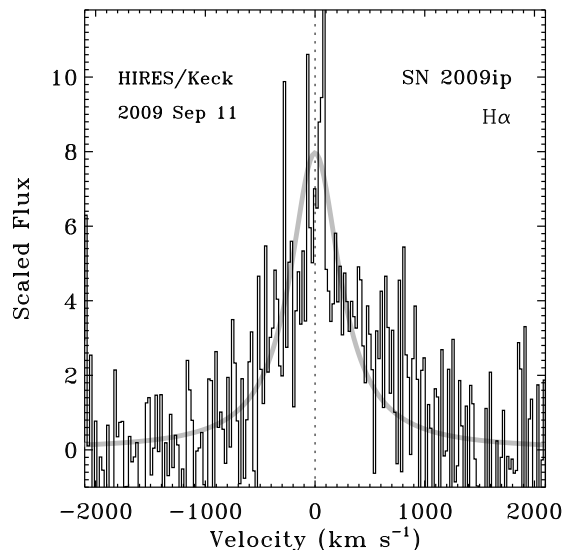


FIG. 7.— HIRES spectrum of SN 2009ip on day 16, showing $H\alpha$. The spectrum has been binned by a factor of 4 to reduce noise, and the continuum was not clearly detected. The thick gray curve is a Lorentzian profile with $\text{FWHM} = 550$ km s^{-1} .

larity of progression.”

To continue quoting Herschel: “What origin can we ascribe to these sudden flashes and relapses?” This old mystery persists, and is made even more extreme by the case of SN 2009ip. A fading of over 3 mag in 16 days is too fast for most physical mechanisms one can imagine, and is faster than most SNe. It cannot be a huge increase in extinction caused by a simple puff of dust formation, since the time for ejected material to reach the dust sublimation radius of 170–230 AU (for the observed luminosity of $\sim 2 \times 10^7 L_{\odot}$) expanding at ~ 500 km s^{-1} is much longer — roughly 600–800 days depending on

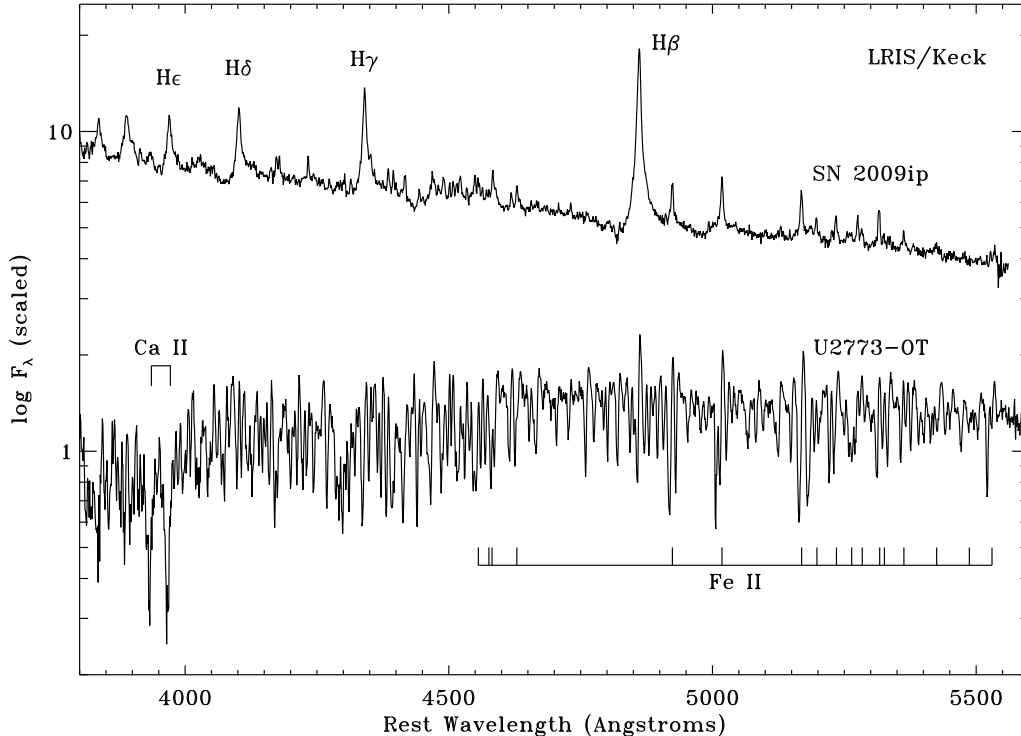


FIG. 8.— Medium-resolution LRIS spectra of SN 2009ip (day 25) and U2773-OT (day 34) in the blue, dereddened by $E(B - V)$ values of 0.019 mag and 0.564 mag for SN 2009ip and U2773-OT, respectively. The forest of absorption lines in U2773-OT is real.

grain-condensation temperatures. We can rule out substantial dust anyway, based on the lack of IR excess during the fading, as discussed below in §3.5. Furthermore, after the dip, the luminosity of SN 2009ip recovered faster than can be explained by the subsequent thinning of that hypothetical dust. One can imagine that hydrogen in the high-density wind could recombine quickly, but this requires that the source of ultraviolet (UV) photons was suddenly quenched, and it seems inconsistent with our detection of $H\alpha$ during the dip. Unless it was much hotter than typical LBV eruptions, the photospheric radius of SN 2009ip must have been comparable to the orbit of Saturn, but fluctuating as fast as (or faster than) the wind’s expansion speed, so the sudden ejection of an optically thick shell is perhaps the most likely culprit. Davidson & Humphreys (1997) noted that in the case of η Car, this rapid fluctuation challenges even the dynamical timescale of the star itself. A fading by more than a factor of 10 over such a short time in SN 2009ip is truly spectacular.

Other LBVs show qualitatively similar fading and re-brightening episodes, although less extreme, which we refer to as “flickering.” V12 in NGC 2403, for example, oscillated wildly in the decade before its eruption (Fig. 3), as noted above, with several changes of more than 1 mag on equally short timescales (Tammann & Sandage 1968). In the same galaxy, V37/SN 2002kg had a rapid fading and re-brightening episode about 350–380 days after peak, as plotted in Figure 4 (see Van Dyk et al. 2006). This sort of rapid variability argues that short cadences are valuable when obtaining photometry and spectroscopy of these objects, lest one miss a significant mass-loss event. In that case, our method of stacking seasonal data for the prediscovery variability of U2773-

OT may have been an oversimplification, which is why we also plot individual measurements in Figures 3 and 4.

3.3. Spectral Morphology

Figures 8 and 9 show the medium-resolution Keck/LRIS spectra at blue and red wavelengths, respectively, of SN 2009ip (day 25) and U2773-OT (day 34). These are useful for discussing the general appearance of the spectra, and the differences between the two transients. We describe the spectral morphology in detail below; in brief, SN 2009ip resembles typical spectra of LBVs in their hotter state, whereas U2773-OT is exemplary of the complex spectra of LBVs in their cooler state.

The day 25 spectrum of SN 2009ip in Figures 8 and 9 is dominated by strong Balmer lines with Lorentzian FWHM widths of $\sim 550 \text{ km s}^{-1}$ and a smooth continuum with an apparent blackbody temperature of $\sim 10^4 \text{ K}$. It also shows broad emission profiles of He I $\lambda\lambda 5876, 6678, \text{ and } 7065$ with similar widths (note that He I $\lambda 5876$ was in the gap between the blue and red LRIS medium-resolution spectra in Figs. 8 and 9, but it can be seen in the low-resolution spectrum in Fig. 12). SN 2009ip also exhibits several narrower emission lines which are mostly Fe II, probably produced in the outer wind. Overall, the spectrum is typical of classical LBVs in their hotter states (e.g., Hillier et al. 2001; Szeifert et al. 1996; Stahl et al. 1993; Stahl 1986). In the dereddened low-resolution day 25 spectrum of SN 2009ip (Fig. 13), we measure a Balmer decrement of $H\alpha : H\beta : H\gamma = 2.74 : 1.0 : 0.48$. This is very close to Case B recombination values, and is similar to the decrement $H\alpha : H\beta : H\gamma = 2.6 : 1.0 : 0.5$ observed in SN 1997bs (Van Dyk et al. 2000) in a spectrum taken shortly after discovery. Note, however, that the spec-

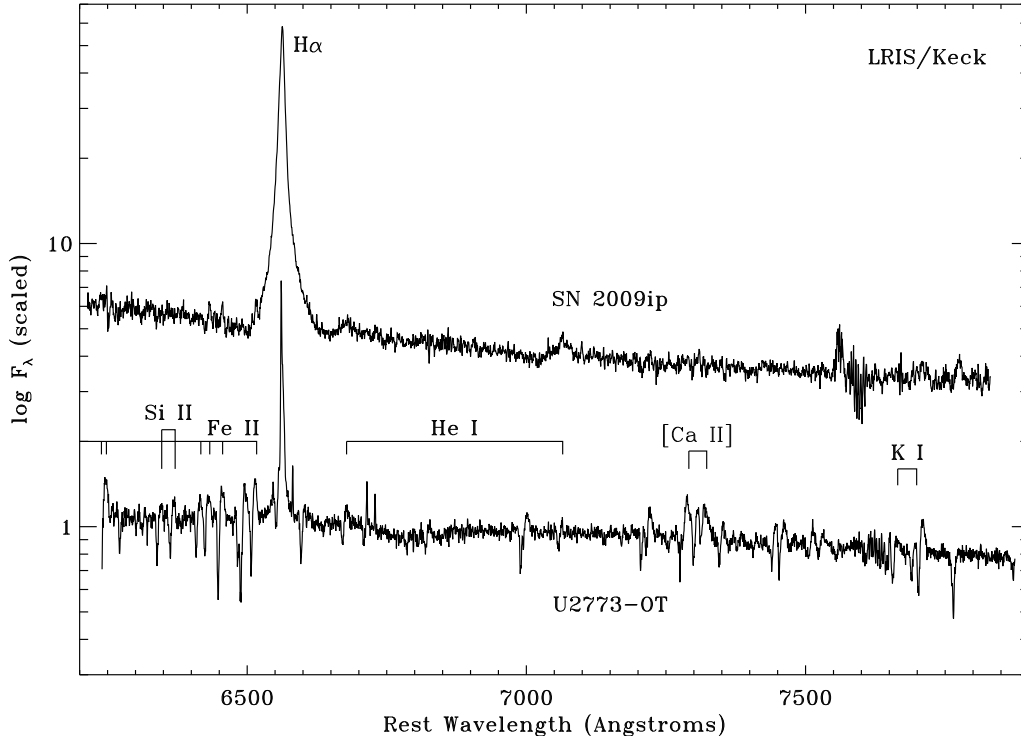


FIG. 9.— Medium-resolution LRIS spectra of SN 2009ip (day 25) and U2773-OT (day 34) in the red, dereddened by $E(B - V)$ values of 0.019 mag and 0.564 mag for SN 2009ip and U2773-OT, respectively.

tral evolution of well-studied SNe IIn such as SN 1994W and SN 2006gy (Chugai et al. 2004; Smith et al. 2010) shows that the Balmer decrement is highly time dependent, steepening as the emitting layer expands, thins, and cools. This may be the case in SN 2009ip as well.

By contrast, the day 34 spectrum of U2773-OT is more complicated, with narrower emission lines, numerous narrow blueshifted absorption lines, and a cooler apparent temperature of ~ 7000 K (this is corrected only for Galactic reddening, so the intrinsic temperature may be somewhat warmer). The prominent absorption indicates that the eruption wind of U2773-OT has lower ionization than that of SN 2009ip. Like SN 2008S and N300-OT, it exhibits strong and narrow emission from [Ca II] $\lambda 7291$ and $\lambda 7323$, as well as bright narrow emission and P Cygni absorption in the near-IR Ca II triplet (the near-IR Ca II triplet is shown in Fig. 13), plus strong absorption in Ca II H and K (Fig. 13). He I lines, if present, are extremely weak. Among the unusual low-ionization P Cygni emission features present in the spectrum of U2773-OT are the K I $\lambda 7665$ and $\lambda 7699$ resonance lines, rarely seen in emission except in cases such as the extreme supergiant VY CMa (e.g., Smith 2004, and references therein). (Note that K I $\lambda 7665$ probably suffers heavier telluric absorption than $\lambda 7665$.) Except for H α , the higher-order Balmer lines are not prominent, while the overall appearance of the spectrum is dominated by a dense forest of narrow absorption lines in the blue, mostly Fe II and other low-ionization metal lines; many of the same lines are seen in emission in SN 2009ip. Interestingly, many of the same emission/absorption features are identified in the spectrum of the Type IIn SN 2006gy (Smith et al. 2010), from which the line identifications in Figures 8 and 9 have been taken, although the lines

in that object are broader. Similarly, many of the same lines are seen in the spectrum of IRC+10420 (Humphreys et al. 2002), although in that object the outflow is slower.

Altogether, the spectrum of U2773-OT is a composite of an emission-line wind spectrum and a dense absorption spectrum of an F supergiant, as is characteristic for LBVs in their cool eruptive states. In fact, its spectrum is an apparent carbon copy of the spectra of R 127 and S Doradus in their cool eruptive states (Wolf 1989; Wolf & Stahl 1990; Wolf et al. 1988; Walborn et al. 2008), for which detailed models suggest a temperature of ~ 8000 K. Armed with this spectrum of U2773-OT and no other data, an informed spectroscopist would conclude that it is most likely an LBV in a cool S Dor phase (see, e.g., Humphreys & Davidson 1994).

Given the stark differences displayed by the spectra of SN 2009ip and U2773-OT in Figures 8 and 9, how can they both be LBVs? The LBVs are a heterogeneous group, but they are known for the duality of their hot (usually quiescent) and cool (outburst) S Dor states. These two preferred states are demonstrated well by each of the two transients in Figures 8 and 9. Interestingly, one can find examples where the same star observed at different points in its variability cycle had a spectrum that resembled that of either SN 2009ip or U2773-OT, such as the case of R 127 (Wolf 1989; Walborn et al. 2008). It may seem puzzling, then, why SN 2009ip is in a hotter spectroscopic state when photometry of the object clearly shows it in mid-eruption. While this behavior is well established for normal S Dor outbursts, we do not yet fully understand the spectroscopic behavior of giant LBV eruptions because spectra of true giant eruptions of LBVs are rare. SN 2009ip clearly indicates that an LBV can be hotter than 8000 K during a giant eruption, as is

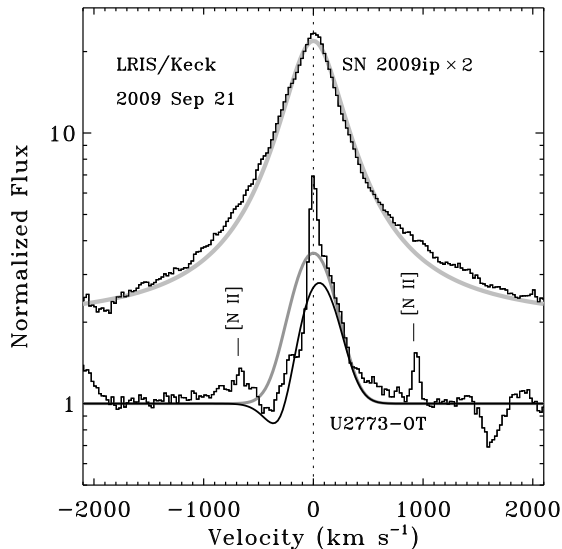


FIG. 10.— Same as Figure 6, but with the medium-resolution LRIS spectra of both U2773-OT and SN 2009ip. The Gaussian curves for U2773-OT are the same velocities as in Figure 6, although with somewhat higher intensities. The gray curve matched to the $H\alpha$ profile of SN 2009ip is a Lorentzian profile with FWHM = 550 km s^{-1} .

apparently the case for SN 1997bs (Van Dyk et al. 2002) and V1 in NGC 2363 (Drissen et al. 2001).

3.4. Emission-Line Profiles and Outflow Speeds

3.4.1. U2773-OT

Figure 6 shows a portion of the spectrum surrounding $H\alpha$ from the Keck/HIRES observation of U2773-OT obtained on day 22 after discovery. The spectrum clearly shows narrow components of $H\alpha$ and the red [N II] lines, plus a broader underlying P Cygni profile in $H\alpha$. The total equivalent width of $H\alpha$ (narrow plus broad) is only $-25.4 \pm 0.3 \text{ \AA}$.

The underlying broad $H\alpha$ P Cygni component can be approximated by an emission component with Gaussian FWHM $\approx 360 \text{ km s}^{-1}$ (gray curve in Fig. 6), plus a Gaussian absorption component that causes the P Cygni minimum at -350 km s^{-1} . This assessment based on the day 22 HIRES spectrum is consistent with the $H\alpha$ profile of U2773-OT observed on day 34 with LRIS (Fig. 10). This weak underlying broad component also matches the expansion speeds observed by Berger & Foley (2009) about 8 days earlier, although they noted this characteristic speed in the P Cygni absorption in the near-IR Ca II triplet and the full emission FWHM of $H\alpha$. We take 350 km s^{-1} to be the expansion speed of the eruption wind from U2773-OT. It is a typical speed for the winds of blue supergiants and LBV stars, but would be astonishingly slow for any conventional explosion scenario. In particular, it is comparable to the 300 km s^{-1} wind observed spectroscopically in the LBV eruption V1 in NGC 2363 (Drissen et al. 2001), which we mentioned earlier, as well as 370 km s^{-1} in V37/SN 2002kg (Van Dyk et al. 2006).

The narrow $H\alpha$ and [N II] features have Gaussian FWHM $\approx 49 \text{ km s}^{-1}$. The red [S II] doublet is also detected with the same line width (not shown). The narrow lines present in the HIRES extracted spectrum seem to indicate an underlying H II region, although 49 km s^{-1} is quite broad for a simple H II region, so these lines may

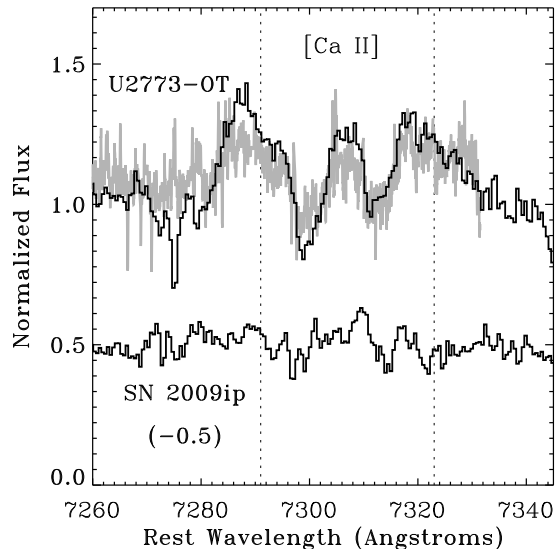


FIG. 11.— LRIS spectra of U2773-OT and SN 2009ip in the wavelength range of the [Ca II] $\lambda\lambda 7291, 7325$ lines (histograms). The spectra are normalized, and SN 2009ip has a value of 0.5 subtracted for display. The noisy gray spectrum is the HIRES spectrum of U2773-OT on day 22, in which the [Ca II] lines fell near the edge of an echelle order. The widths of the lines in U2773-OT are consistent with the 350 km s^{-1} FWHM of $H\alpha$.

also arise in an extended circumstellar nebula ejected by the star in a previous outburst. This narrow emission was also seen and spatially resolved in our LRIS spectra, but the extended emission along the slit and the good seeing allowed us to carefully subtract it. Some [N II] residuals remain in Figure 10, but the narrow lines are considerably weaker than in Figure 6. In these narrow lines, the observed [S II] F_{6716}/F_{6731} ratio is ~ 1.2 , corresponding to a fairly low electron density of $\sim 120 \text{ cm}^{-3}$ (e.g., Osterbrock 1989). The presence of an H II region coincident with U2773-OT supports the hypothesis that the progenitor of U2773-OT was a young, massive star. Both η Car and V1 in NGC 2363 are also located within bright, giant H II regions. On the other hand, if this narrow emission arises in part from extended circumstellar material, the [N II] lines and other features are reminiscent of extended LBV nebulae, which tend to be enriched in N (Stahl 1987; Stahl 1989; Stahl & Wolf 1986).

Finally, we show the spectrum in the region of the [Ca II] lines in Figure 11. These lines were first noted to be strong by Berger & Foley (2009) on day 16. Figure 11 indicates that the [Ca II] lines are detected in both the HIRES spectrum (day 22) and the LRIS spectrum (day 34) as well. The lines have width of roughly 350 km s^{-1} , comparable to $H\alpha$, although the lines are irregularly shaped, so accurate FWHM values are difficult to determine. Another unidentified emission line appears to be seen between the two [Ca II] lines.

3.4.2. SN 2009ip

Figure 10 shows the $H\alpha$ profile of SN 2009ip in the medium-resolution LRIS spectrum, obtained on day 25 just after it recovered from its sharp 3 mag dip. This is superior to the HIRES spectrum on 2009 Sep. 11 (Fig. 7), which had low S/N because it was obtained during the sharp dip. The $H\alpha$ line is extremely bright, with a total emission equivalent width of -198 \AA , and a flux of $2.1 \times 10^{-14} \text{ erg s}^{-1} \text{ cm}^{-2}$. (This line flux is 3 times

brighter than measured in the HIRES spectrum.) This corresponds to a total $H\alpha$ line luminosity of $\sim 2.5 \times 10^5 L_{\odot}$. The $H\alpha$ line profile is qualitatively similar several days earlier in the HIRES spectrum obtained during the dip, but the line flux is weaker.

The $H\alpha$ line in SN 2009ip is clearly broader than that of U2773-OT, and it is symmetric, unlike the P Cygni absorption profile seen in U2773-OT. In order to fit the symmetric profile, one would need a composite Gaussian with a broad, intermediate, and narrow component. However, the line profile is fit quite naturally with a single Lorentzian profile with $\text{FWHM} = 550 \text{ km s}^{-1}$. The same Lorentzian profile adequately accounts for $H\alpha$ in the HIRES spectrum, although that spectrum has a much higher noise level. As discussed in detail by Smith et al. (2010) for SN 2006gy, a Lorentzian profile is probably indicative of multiple electron scattering through an opaque wind, suggesting a very high mass-loss rate for the SN 2009ip eruption. Although the $H\alpha$ line wings extend to roughly $\pm 2000 \text{ km s}^{-1}$ at zero intensity, the Lorentzian profile suggests that these are electron-scattering wings and not true kinematic speeds of outflowing material.

We therefore adopt 550 km s^{-1} as the characteristic outflow speed of SN 2009ip, in agreement with the earlier assessment by Berger et al. (2009b), although they did not specifically mention the Lorentzian profile. This speed is faster than the $300\text{--}370 \text{ km s}^{-1}$ expansion observed in U2773-OT, V1 in NGC 2363 (Drissen et al. 2001), and V37/SN 2002kg (Van Dyk et al. 2006), and it is closer to the 600 km s^{-1} outflow speed around more massive LBVs like the Homunculus of η Car (Smith 2006). Despite this connection, it is unclear if there is a trend of higher outflow speeds in more luminous objects, because the outflow speeds were even higher in SN 2008S and N300-OT, where the progenitors were less luminous. In Figure 11 we also show the medium-resolution LRIS spectrum in the wavelength range corresponding to the red [Ca II] lines, plotted along with the same wavelength range in U2773-OT. It is clear that the [Ca II] lines are not detected in SN 2009ip.

3.4.3. Fast Ejecta and a Blast Wave?

Most spectral lines in both transients discussed here agree with the outflow velocities determined from $H\alpha$, discussed above, and we take these to be the dominant outflow speeds for each object. In U2773-OT the characteristic speeds are of order 350 km s^{-1} , while the characteristic speeds of 550 km s^{-1} for SN 2009ip are higher. The $H\alpha$ profile in SN 2009ip does show wings extending to $\pm 2000 \text{ km s}^{-1}$, but these seem consistent with electron-scattering wings in a Lorentzian profile, as discussed above. There are, however, signs of some faster material in SN 2009ip.

Figure 12 shows the region of the spectrum including He I $\lambda 5876$ and the Na I D lines, seen in the low-resolution LRIS spectra of both targets (this spectral window was not included in the blue or red medium-resolution LRIS spectra in Figs. 8 and 9). The Na I D line in U2773-OT shows a narrow P Cygni profile, with an absorption trough consistent with outflow speeds in other lines; there is no sign of He I emission or fast material.

SN 2009ip, on the other hand, shows interesting new

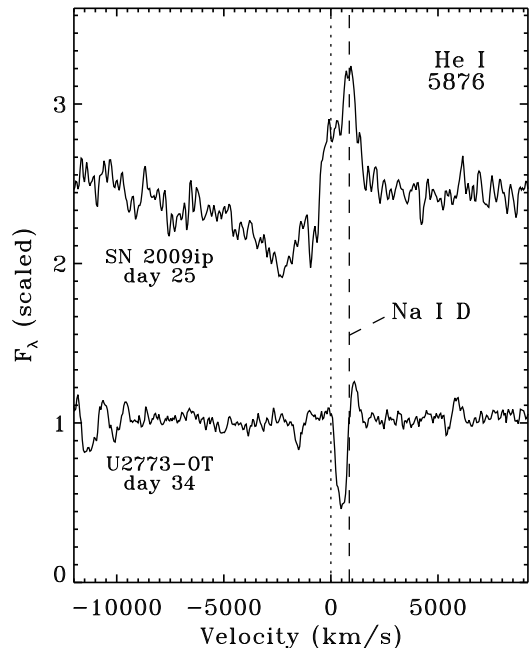


FIG. 12.— Low-resolution LRIS spectra of SN 2009ip and U2773-OT, zooming in on He I $\lambda 5876$ and the Na I D lines (the continuum level in the SN 2009ip spectra has been normalized with a tilted blue continuum). The velocity scale is relative to He I $\lambda 5876$ (dotted line), but the zero-velocity position for Na I D $\lambda 5895$ is shown with the long-dash line for reference. The observed line profile is a combination of both lines, but we suspect that the broad emission and absorption feature in SN 2009ip is mainly He I, superposed with narrow Na I D emission and absorption.

structure in this line. Aside from a narrow emission peak at the systemic velocity of Na I D, the feature is dominated by a broad He I $\lambda 5876$ P Cygni profile. The emission component has a width and wings consistent with other He I lines in the spectrum like $\lambda 6678$ and $\lambda 7065$, as well as the symmetric wings of $H\alpha$. The blueshifted absorption of He I $\lambda 5876$, however, is the only line detected in our spectra that provides clear evidence for faster outflow speeds of roughly $3000\text{--}5000 \text{ km s}^{-1}$.

These outflow speeds seen only in absorption exceed the characteristic speed of 550 km s^{-1} seen in emission lines in the spectrum of SN 2009ip. This is reminiscent of the two ranges of outflow speeds seen in η Car: most of the mass in the Homunculus nebula expands at $500\text{--}600 \text{ km s}^{-1}$ (Smith 2006), whereas recent spectra of faint material exterior to that reveal much faster material moving at $3000\text{--}6000 \text{ km s}^{-1}$ (Smith 2008). The kinematics are consistent with both components originating in the same event in the 1840s, implying that η Car's giant eruption also had a fast blast wave containing a comparable amount of kinetic energy but far less mass than the slower Homunculus nebula (Smith 2008). The fast $3000\text{--}5000 \text{ km s}^{-1}$ material seen in absorption in SN 2009ip, along with the dominant speeds of 550 km s^{-1} in most emission lines, may suggest a similar scenario with a blast wave ahead of the slower ejecta for SN 2009ip. Indeed, the coexistence of narrow components of 550 km s^{-1} along with an intermediate-width component of a few 10^3 km s^{-1} is also reminiscent of the broader class of SNe IIn (see the discussion of line profiles in Smith et al. 2010 and Chugai & Danziger 1994), although the intermediate-width components tend to be stronger in SNe IIn.

If this fast material is evidence for a weak blast wave in SN 2009ip, then there are several interesting implications beyond the connection to η Car. First, shocks can heat material above the equilibrium radiation temperature and may produce additional ionizing radiation, so this might help explain the duality of spectra seen in U2773-OT and SN 2009ip. Namely, it may help explain why SN 2009ip had a relatively hot spectrum, even though super-Eddington LBV eruptions are expected to appear cooler (more like U2773-OT; see Humphreys & Davidson 1994). Second, the existence of a shock on day 25 (during the second peak) may hint that a shock-breakout event could be responsible for the initial rise to peak luminosity and astonishingly sudden decline, whereas the resurgence after the dip might then be explained by the beginning of shock interaction with surrounding circumstellar material, as in standard SNe IIn. A shock breakout has never before been claimed in an LBV eruptive event, and the suggestion is still quite speculative, but it may nevertheless have some application to other events. Unfortunately, we are not able to obtain spectra or multi-band photometry during the initial peak of SN 2009ip, so we cannot determine if the temperature was very high as one might expect from shock breakout, but SN 2009ip warns that we should be on the lookout for this behavior in future LBV eruptions.

3.5. [Ca II] and IR Excess — or Not

Our low-resolution spectra of SN 2009ip and U2773-OT are shown in Figure 13. These were obtained on the same night with Keck/LRIS, and correspond to days 25 and 34 after discovery for SN 2009ip and U2773-OT, respectively. SN 2009ip is dominated by a very blue ($T \approx 10,000$ K) continuum and bright Balmer emission lines, characteristic of LBVs. It is compared to the spectrum of the LBV eruption SN 1997bs in Figure 13. The dereddened low-resolution spectrum of U2773-OT shows a blue continuum as well, with a lower apparent temperature around 7000 K. It also has Balmer emission lines, although much narrower as noted earlier and riddled with many deep blueshifted absorption features indicating an underlying spectrum like an F supergiant with strong wind lines, characteristic of many LBVs (see §3.3), as well as emission from [Ca II] and the Ca II near-IR triplet. The Ca II H & K lines show strong, broad absorption, like SN 2008S and N300-OT. The spectrum of U2773-OT in Figure 13 is similar to those of SN 2008S and IRC+10420 (and by extension, N300-OT), although with somewhat weaker [Ca II] lines, and with more pronounced and more numerous P Cygni absorption features.

Our spectra of SN 2009ip and U2773-OT agree qualitatively with preliminary reports of the spectra. Berger et al. (2009b) obtained a medium-resolution spectrum of SN 2009ip shortly after discovery, and noted that it exhibited narrow (FWHM ≈ 550 km s $^{-1}$) Balmer emission lines, in agreement with our spectrum on day 25. Berger & Foley (2009) obtained spectra of U2773-OT and noted similarly narrow (FWHM ≈ 350 km s $^{-1}$) Balmer emission lines, in agreement with our HIRES and LRIS spectra described above, plus [Ca II], Ca II, and a few other emission features. Taken at face value, one might conclude from these spectral characteristics that U2773-OT is closely related to the recent transients SN 2008S and N300-OT, which were discovered to have unusually

bright [Ca II] emission in their spectra (Smith et al. 2009; Berger et al. 2009a; Bond et al. 2009), whereas SN 2009ip is apparently not.

The other very unusual characteristic shared by SN 2008S and N300-OT is that both had heavily dust-enshrouded progenitors detected only in *Spitzer* data (Prieto 2008; Prieto et al. 2008), and significant dust was still present around both at late times (Prieto et al. 2009; Wesson et al. 2010). Does this connection between [Ca II] emission and dust hold for the two new transients discussed here?

SN 2009ip was detected at ~ 20.2 mag in an unfiltered Keck guider image on 2009 Sep. 11. Assuming this guider image closely approximates the R band, this means the $R-K'$ color was ~ 0.5 mag at this epoch, compared to our near-IR image taken 2 days earlier. Given the fast optical decline of SN 2009ip at this time (~ 2 mag between Aug. 30 and Sep. 11), however, it is likely that $R-K$ was even less than 0.5 mag. Thus, we measure very little if any near-IR excess in SN 2009ip. It must have had little circumstellar dust near the star to cause excess emission or circumstellar extinction, in direct contrast to N300-OT and SN 2008S which had $R-K \approx 3$ mag and ~ 1.7 mag, respectively, at peak optical output (Bond et al. 2009; Botticella et al. 2009). For both of these transients the $R-K$ color evolved redward as they declined.

U2773-OT, on the other hand, does show a considerable near-IR excess. After correcting for Galactic extinction, we find that U2773-OT had $R-K_s \approx 1.5$ mag on 2009 Sep. 8. Figure 5 shows that its near-IR/optical color has remained relatively unchanged since then, as it brightened by ~ 0.2 mag over 100 days. Its near-IR excess is comparable to that of SN 2008S in eruption. Regardless of whether the near-IR color excess is caused by reddening from circumstellar dust or emission from heated dust, the IR excess points to a dusty environment around U2773-OT. (The IR excess might also be caused in part by newly formed dust, although a more detailed study of the evolving spectral energy distribution and line profiles would be needed to investigate this further.)

It therefore appears that U2773-OT did indeed have a substantially dusty circumstellar environment to accompany its [Ca II] emission — like SN 2008S and N300-OT — while SN 2009ip had neither. The dusty environment around the U2773-OT progenitor was not as fully obscuring as the dust around the progenitors of SN 2008S and N300-OT, although in those cases the progenitor obscuration was due mostly to a more compact distribution of dust that seems to have been largely destroyed by their luminous outbursts (Wesson et al. 2010; Prieto et al. 2009), leaving more distant dust shells comparable to that seen now around U2773-OT. The dust around U2773-OT is also reminiscent of the dusty environments inferred around the transients M85-OT and SN 1999bm, which led Thompson et al. (2009) to place those two objects in the same class with SN 2008S and N300-OT.

This is intriguing, since we have shown that *both* SN 2009ip and U2773-OT were otherwise very similar, with pre-eruption LBV variability in the decade before discovery, luminous LBV-like progenitors, and very narrow line widths that were even narrower than those of SN 2008S or N300-OT but characteristic of LBVs. One must therefore conclude that the presence of strong

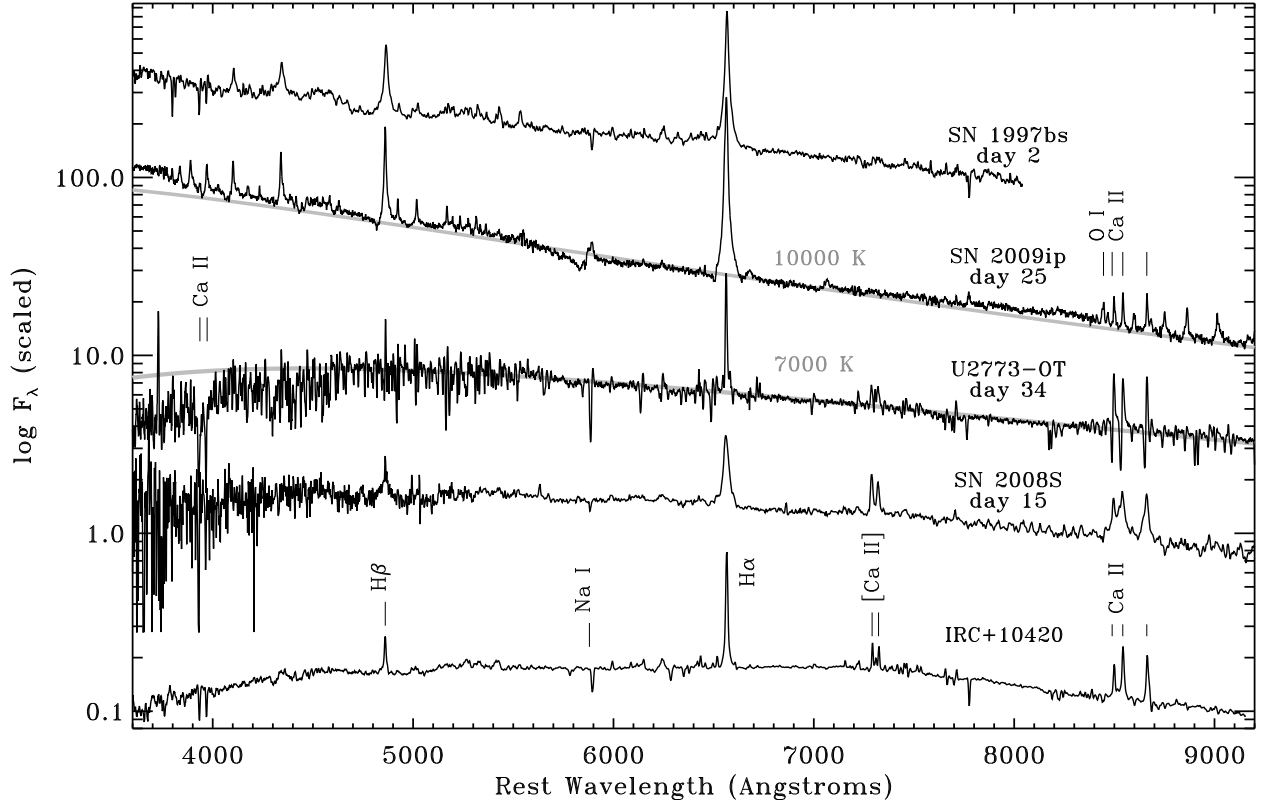


FIG. 13.— Low-resolution LRIS spectra of SN 2009ip and U2773-OT, dereddened by $E(B - V)$ values of 0.019 mag and 0.564 mag, respectively. The continuum slopes of SN 2009ip and U2773-OT are matched by blackbodies with $T = 10,000$ K and 7000 K, respectively. These spectra are compared to optical spectra of SN 2008S and the yellow hypergiant IRC+10420 (from Smith et al. 2009), as well as SN 1997bs (Van Dyk et al. 2002).

[Ca II] and Ca II emission *cannot be taken as evidence for or against an LBV nature*. Instead, [Ca II] emission is more closely related to the progenitor’s circumstellar environment — especially the presence of dust. It was already noted that the bright [Ca II] and Ca II lines in SN 2008 and N300-OT are probably related to dense circumstellar gas and pre-existing circumstellar dust grains that were vaporized by the increased outburst radiation (Prieto et al. 2008; Smith et al. 2009). The corresponding implications for SN 2008S and N300-OT are discussed further in §4.2.

A dusty circumstellar environment around the progenitor of U2773-OT affects our estimates of the progenitor properties, as noted above. From *HST* photometry corrected only for Galactic extinction and reddening, we found that the quiescent progenitor (~ 10 yr before discovery) had a color consistent with that of an early A-type supergiant having a luminosity of $\log(L/L_{\odot}) \approx 5.1$, and an initial mass of roughly $20 M_{\odot}$. With substantial circumstellar dust, the progenitor of U2773-OT must have been even hotter than an early A-type star, and more luminous and massive as well, although one cannot make precise corrections with available information. It is difficult to escape the conclusion that U2773-OT was blue, quite luminous, and obviously highly variable, so it was therefore likely to have been an LBV. Its spectral morphology confirms this. Conversely, there was little pre-existing circumstellar dust around SN 2009ip, which is reassuring because its quiescent progenitor with $M \approx -10$ mag would already be among the most lu-

minous stars known, and any significant amount of dust would raise the corresponding progenitor luminosity.

4. DISCUSSION

4.1. Precursor *S Doradus* Eruptions

A critical new result from this study is that we have recovered the luminous progenitor stars and precursor variability in the decade preceding the discovery of SN 2009ip and U2773-OT, and that the luminosity and variability are characteristic of known LBVs like η Car, SN 1954J (V12), and V1 in NGC 2363. Before these precursor outbursts began, the two stars were apparently at quiescent absolute magnitudes of -8.0 to -10 mag, implying moderately massive and very massive progenitor stars for U2773-OT and SN 2009ip, respectively.

We propose that the apparent brightening episodes in the ~ 10 yr before the giant LBV eruptions of SN 2009ip and U2773-OT were caused by preparatory outburst phases, akin to S Dor-like variability, which then grew into giant eruptions as is thought to be the case for the precursor behavior of η Car and SN 1954J (Humphreys et al. 1999). SN 1961V may have also been in an S Dor phase for 10–20 yr preceding its giant eruption (Goodrich et al. 1989).

The visual brightening identified as S Dor outbursts, named for the famous prototype LBV star in the Large Magellanic Cloud, occurs when the star varies at roughly constant M_{Bol} , but brightens roughly 1–2.5 mag at visual wavelengths because it becomes cooler, redistributing its peak flux from the UV to visual wavelengths (see

Humphreys & Davidson 1994). S Dor outbursts are a *defining* observed phenomenon in LBVs, although not every S Dor phase is followed by a giant eruption. The namesake of the class, for example, has never been observed in a giant eruption, but only smaller oscillations. The situation can be more complicated as well: S Dor-like variability may evolve into larger outbursts. For example, the 1990s eruption of V1 in NGC 2363 may not have been a simple S Dor phase, because its bolometric luminosity increased (Drissen et al. 2001), and we should be mindful that this may be the case for our two new transients discussed here as well. In any case, LBVs exhibit a wide variety in ΔM_V and Δt , but a few to 10 yr is a typical observed timescale for these S Dor variations (see Humphreys & Davidson 1994; van Genderen 2001).

As noted earlier, neither S Dor outbursts nor giant LBV eruptions have a theoretical explanation, although they are suspected to be the result of luminous stars flirting with an opacity-modified Eddington limit and subsequent runaway mass loss (e.g., Smith & Owocki 2006; Humphreys & Davidson 1994; Smith et al. 2003; Owocki et al. 2004). SN 2009ip and U2773-OT are important in this context because they add two new well-observed cases to the three historical examples of precursor variability before a giant LBV eruption, and unlike the historical examples, we also have obtained spectra of their eruptions which resemble other recent SN impostors without documented pre-eruption LBV-like variability.

Given the stark differences from one object to the next, and the presence of “preparatory” precursor outbursts in the decade preceding maximum light for some objects, one wonders to what extent there is cumulative hysteresis built into the system. For example, to what extent does the peak luminosity output and rate of decline depend systematically on the pre-eruption variability and its associated mass loss? At this time such questions are still quite speculative, but a larger sample of these transients with good observations would obviously be valuable to establish any such trends.

4.2. Implications for SN 2008S and N300-OT

The spectrum of one object we discussed here, U2773-OT, resembles the optical spectra of SN 2008S, N300-OT, and IRC+10420, as noted above. The other, SN 2009ip, matches spectra of SN impostor LBVs like SN 1997bs that are dominated by Balmer lines alone. Yet, based on the luminous progenitors and their S Dor variability, we have identified *both* SN 2009ip and U2773-OT as giant LBV eruptions.

This link reinforces earlier suggestions that SN 2008S and N300-OT may also have been related to LBV-like eruptions, albeit with relatively low-luminosity (and possibly cooler) dust-obscured progenitors. It also suggests that some giant LBV eruptions have bright [Ca II] and Ca II emission lines while some do not. Several authors have noted that the bright [Ca II] and Ca II lines are probably related to dense circumstellar gas and the destruction of dust grains (Prieto et al. 2008; Smith et al. 2009; this work). In the case of IRC+10420, this dust destruction¹⁰ occurs because the star has been growing much warmer over the past 30 years, and increasing its UV

output (see Smith et al. 2009; Humphreys et al. 2002). In the transients, it occurs because of the sudden increase in luminosity that pushes the grain sublimation radius farther into the progenitor’s dust shell.

Among known LBVs, some are dusty, and some are not. Some have no detected circumstellar shells, while others like η Car have 15 M_\odot dust shells (Smith et al. 2003) that reprocess nearly all of the star’s UV and visual radiation. The difference depends on the star’s previous mass-loss history (i.e., how recently it has ejected a massive dust shell, and how fast that dust shell expands and thins). Regardless of its initial mass, a star that has recently suffered an LBV-like eruptive event could be completely obscured at optical wavelengths, while its IR/optical colors would evolve rapidly over the subsequent century. The obscured phase could be very brief and mostly missed in samples of known LBVs, in agreement with the expected short duration implied by the rarity of similar dust obscured stars (Thompson et al. 2009). If strong [Ca II] emission is indeed linked to vaporizing circumstellar dust, then it would not be surprising to have some giant LBV eruptions with strong [Ca II] emission and some with only weak emission or none. For example, Valeev et al. (2009) recently reported a new LBV in M33, which has a dust shell and bright [Ca II] emission.

Another key issue is the variability of the progenitors. The lack of IR variability in the progenitors of SN 2008S and N300-OT seems problematic for their interpretation as EAGB stars that become ecSNe. All stars at the tip of the AGB pulsate with large amplitudes (e.g., Mira variables). Thompson et al. (2009) demonstrated clearly that over timescales of a few years in the same IRAC bands, known EAGB stars are highly variable ($\Delta M_{4.5}$ is typically ~ 1 mag), whereas LBV candidates with dust shells are not highly variable (a few exceptions have $\Delta M_{4.5}$ as much as 0.5 mag). One reason for this is that although LBVs are variable at visual wavelengths during S Dor-like episodes, their *bolometric* luminosity remains roughly constant. Recall that the observed visual-wavelength brightening in S Dor outbursts is thought to be a redistribution of flux from the UV to optical — i.e., a change in bolometric correction at constant luminosity. Since the dust properties depend primarily on the central engine’s bolometric output, one may expect the mid-IR luminosity of a circumstellar dust shell around an LBV to be nearly constant — that is, until it experiences a giant eruption when the bolometric luminosity actually climbs.

SN 1954J/V12 is a key example to keep in mind when debating the nature of SN 2008S and N300-OT, because it is a well-established LBV, but its luminosity was comparable to the relatively low luminosities of the two dust-enshrouded transients. The two new sources we report here appear to bridge the gap between these examples and more luminous LBVs. If SN 2008S and N300-OT were blue supergiants that were heavily obscured by dust, then the initial masses implied by their IR luminosities

related to SN 2008S and N300-OT. In fact, IRC+10420 is heavily enshrouded by circumstellar dust, with most of its luminosity escaping at 10–20 μm (e.g., Humphreys et al. 1997). Although IRC+10420 is more luminous, the ratio between its 8 μm and optical *R*-band flux is similar to the observed colors of SN 2008S and N300-OT.

¹⁰ Botticella et al. (2009) stated that IRC+10420 is not enshrouded by a dust shell to support their claim that it is not

are higher than if one assumes that they are at the tip of an ascending AGB/RSG branch. One cannot confidently determine the effective temperature or color of an underlying star from the mid-IR dust emission properties; for example, in the mid-IR color plots presented by Thompson et al. (2009), η Car had the same *Spitzer* colors as the very cool red supergiant VY CMa. Altogether, then, we find the case to be still quite plausible that SN 2008S and N300-OT may have been eruptions analogous to episodic LBV-like events, at lower initial masses than had previously been recognized. The variety among this class of objects may be telling us that episodic mass loss and eruptive phenomena are a generic property of late evolutionary phases over a wide range of initial masses, whatever the underlying cause.

Still, there are some key differences between LBVs and SN 2008S/N300-OT which remain unsolved even if these are not episodic LBV-like eruptions. One is the apparently C-rich chemistry in the circumstellar dusty envelope of N300-OT (Prieto et al. 2009). Non-silicate dust was also inferred for SN 2008S (Wesson et al. 2010). Massive stars are generally not found to be C-rich for long periods except in the WC Wolf-Rayet phase, providing the most compelling argument made for a connection to EAGB stars (Prieto et al. 2009; Thompson et al. 2009). This is puzzling as well, though, since C-rich AGB stars are thought to come from lower-mass stars (Jura 1991), well below the N300-OT progenitor mass of 12–25 M_{\odot} inferred by Gogarten et al. (2009). Furthermore, the C enrichment in single carbon stars is thought to arise from dredge up during unstable He shell burning over a degenerate C-O core. One expects progenitors of ec-SNe to avoid this enrichment, however, because they do not make a degenerate C-O core, instead burning carbon to eventually produce the O-Ne-Mg core that collapses (e.g., Nomoto 1984). With such mysteries, one may feel tempted to appeal to previous episodes of mass transfer in evolved close binary systems for any plausible initial mass range. It is worth noting, however, that observations of the dust composition in η Car (Chesneau et al. 2005; Mitchell & Robinson 1978; Smith 2010) have also shown strong evidence for unusual non-silicate dust, such as corundum (Al_2O_3) and other species. The unusual grain composition may be related to the *rapid* formation of dust around a hot star, where condensation temperature may compete with chemical abundances in determining the grain composition (e.g., Smith 2010). In other words, the presence of carbon dust may not necessarily result directly from carbon-rich gas-phase abundances. For many other LBVs, the dust composition has not been studied in detail yet, so an attempt to detect or rule out the presence of carbon-bearing dust or molecules would be interesting.

5. CONCLUSIONS

We have investigated the two recent transients SN 2009ip and U2773-OT. While they show some spectral differences, we conclude that they are two manifestations of the same underlying phenomenon: namely, they are both giant eruptions of luminous blue variables (LBVs). Here we briefly summarize the main conclusions of our study.

(1) The quiescent progenitor stars of both transients have been identified in *HST* images taken ~ 10 yr before

discovery. The progenitor of SN 2009ip was an extremely luminous star with $M_V \approx -9.8$ mag, $\log(L/L_{\odot}) = 5.9$, and a probable initial mass of 50–80 M_{\odot} . This places it well above the observed upper limit for red supergiants, so it was either a yellow or blue supergiant. The progenitor of U2773-OT was somewhat less luminous, at $M_V \approx -7.8$ mag and $\log(L/L_{\odot}) = 5.1$, corresponding to an initial mass of $\sim 20 M_{\odot}$. It had an observed color similar to that of an early A-type supergiant, consistent with lower-luminosity LBVs. However, an IR excess reveals that U2773-OT had a dusty environment, so it was most likely hotter, more luminous, and more massive, also consistent with an LBV.

(2) Examining pre-discovery ground-based data, we discovered a long ~ 5 yr history of LBV-like photometric variability in the decade leading up to the peaks of eruption for both transients. The precursor variability resembles the preparatory S Dor phases that transformed into giant LBV eruptions of η Car, SN 1954J, and SN 1961V. We suspect that this early warning sign is an important key for triggering a giant eruption, although many S Dor phases do not result in a giant eruption, and it is unclear if all giant eruptions show precursor outbursts.

(3) Immediately after reaching its peak, we discovered that SN 2009ip took a sharp dive, fading by 3.2 mag in 16 days, followed by an almost immediate recovery to nearly its previous level. The astonishing decline rate is faster than that of SNe, and the recovery is unprecedented. The closest analog is the visual light curve of η Car during its 1843 Great Eruption. This would suggest that SN 2009ip is physically related to η Car, and we should not be surprised if its eruption continues. After reaching its peak level, U2773-OT seems to have sustained a relative plateau, with only minor variations at the time of writing.

(4) Optical spectra of the two transients are qualitatively different, but each is characteristic of LBVs at different phases of their variability. SN 2009ip is dominated by very strong Balmer emission lines and outflow speeds of $\sim 550 \text{ km s}^{-1}$, similar to η Car. Evidently, SN 2009ip did not show a cool photosphere, counter to some expectations for LBV eruptions. U2773-OT has a cooler 7000–8000 K spectrum of an F supergiant superposed with wind emission lines and sharp blueshifted absorption features, indicating an outflowing wind of 350 km s^{-1} . It is almost identical to the spectrum of S Dor and other LBVs in their cool eruptive phases. This dichotomy illustrates the wide variety of spectral properties that can be observed in LBV eruptions.

(5) SN 2009ip also shows evidence for fast material moving at 3000–5000 km s^{-1} seen in absorption of He I $\lambda 5876$. These speeds are much faster than most of the mass traced by emission lines (550 km s^{-1}), and this combination is quite reminiscent of the slower Homunculus and fast blast wave of η Car (Smith 2008). We speculate that shock excitation by this fast blast wave may play a role in giving rise to the hotter spectrum of SN 2009ip, and may be related to the sharp initial peak in the light curve.

(6) The spectrum of U2773-OT has [Ca II] emission and other features reminiscent of the recent transients SN 2008S and N300-OT, as well as an IR excess indicating a dusty environment. SN 2009ip has neither of

these attributes, yet both are clearly LBVs. This illustrates that the diversity of LBV circumstellar environments can give rise to a wide range of properties such as those seen in SN 2008S and N300-OT, depending on the star's recent mass-loss history.

(7) We have noted that the progenitor luminosities for some LBVs are much lower than that of η Car, such as U2773-OT, SN 1954J/V12, and V1 in NGC 2363, all of which imply initial masses around $20 M_{\odot}$. The progenitor luminosities of these well-established LBVs overlap with the low IR luminosities of the dust-obscured progenitors of SN 2008S and N300-OT, adding weight to the possibility that these are moderately massive stars of 12–15 M_{\odot} that experienced eruptive instability analogous to LBVs.

We thank an anonymous referee for critical comments that helped improve the manuscript. Some of the data presented herein were obtained at the W. M. Keck Observatory, which is operated as a scientific partnership among the California Institute of Technology, the University of California, and NASA; the observatory was made possible by the generous financial support of the W. M. Keck Foundation. We thank the Lick and Keck Observatory staffs for their dedicated help, and we acknowledge Chris Fassnacht for assistance with obtaining flatfields for the NIRC2 obser-

vations. We are grateful to Cullen Blake, Dan Starr, and Mike Strutskie for their help with the development and operations of PAIRITEL. In addition, we appreciate the assistance and patience of Ryan Foley, Armin Rest, and Dan Kasen during the Keck/LRIS observing run when we discovered the rebrightening of SN 2009ip. The supernova research of A.V.F.'s group at U.C. Berkeley is supported by National Science Foundation (NSF) grants AST-0607485 and AST-0908886, the TABASGO Foundation, and the Richard & Rhoda Goldman Fund. Financial support for this work was also provided by NASA through grant AR-11248 from the Space Telescope Science Institute, which is operated by Associated Universities for Research in Astronomy, Inc., under NASA contract NAS 5-26555. KAIT and its ongoing operation were made possible by donations from Sun Microsystems, Inc., the Hewlett-Packard Company, AutoScope Corporation, Lick Observatory, the NSF, the University of California, the Sylvia & Jim Katzman Foundation, and the TABASGO Foundation. J.S.B. and A.A.M. were partially supported by a NASA/*Swift* Guest Investigator (Cycle 5) grant and a SciDAC grant from the U.S. Department of Energy. This research used data products from the Two Micron All Sky Survey, which is a joint project of the University of Massachusetts and the Infrared Processing and Analysis Center/California Institute of Technology, funded by NASA and the NSF. It also used resources of the National Energy Research Scientific Computing Center, which is supported by the Office of Science of the U.S. Department of Energy under Contract No. DE-AC02-05CH11231; P.E.N. thanks them for a generous allocation of computing time and space on their machines in support of DeepSky.

Facilities: *HST* (WFPC2), Keck I (LRIS, HIRES), Keck II (NIRC2/LGSAO), Lick (KAIT), PAIRITEL

REFERENCES

- Berger, E., & Foley, R. J. 2009, ATel, 2187, 1
 Berger, E., Foley, R. J., & Ivans, I. 2009b, ATel, 2184, 1
 Berger, E., et al. 2009a, ApJ, 699, 1850
 Bloom, J. S., et al. 2006, in *Astronomical Data Analysis Software and Systems XV*, ed. C. Gabriel, et al. (San Francisco: ASP), 751
 Boles, T. 2009, CBET, 1931, 1
 Bond, H., et al. 2009, ApJ, 695, L154
 Botticella, M. T., et al. 2009, MNRAS, 398, 1041
 Chesneau, O., et al. 2005, A&A, 435, 1043
 Chu, Y. H., et al. 2004, AJ, 127, 2850
 Chugai, N.N., & Danziger, I.J. 1994, MNRAS, 268, 173
 Davidson, K., & Humphreys, R. M. 1997, ARAA, 35, 1
 Dolphin, A. E. 2000a, PASP, 112, 1383
 Dolphin, A. E. 2000b, PASP, 112, 1397
 Drissen, L., Roy, J. R., & Robert, C. 1997, ApJ, 474, L35
 Drissen, L., Crowther, P. A., Smith, L. J., Robert, C., Roy, J. R., & Hillier, D. J. 2001, ApJ, 546, 484
 Filippenko, A. V. 2003, in *From Twilight to Highlight: The Physics of Supernovae*, ed. W. Hillebrandt & B. Leibundgut (Berlin: Springer-Verlag), 171
 Filippenko, A. V., Barth, A. J., Bower, G. C., Ho, L. C., Stringfellow, G. S., Goodrich, R. W., & Porter, A. C. 1995, AJ, 110, 2261
 Filippenko, A. V., Li, W. D., Treffers, R. R., & Modjaz, M. 2001, in *Small-Telescope Astronomy on Global Scales*, ed. W. P. Chen, C. Lemme, & B. Paczyński (San Francisco: ASP), 121
 Frew, D. J. 2004, J. of Astron. Data, 10, 6
 Goodrich, R. W., Stringfellow, G. S., Penrod, G. D., & Filippenko, A. V. 1989, ApJ, 342, 908
 Herschel, J. F. W. 1847, in *Results of Observations Made During the Years 1834-1888 at the Cape of Good Hope* (London: Smith Elder), 32
 Hillier, D. J., et al. 2001, in *Eta Carinae & Other Mysterious Stars*, ed. T. Gull, S. Johansson, & K. Davidson (San Francisco: ASP), 15
 Hubble, E., & Sandage, A. 1953, ApJ, 118, 353
 Humphreys, R. M., & Davidson, K. 1994, PASP, 106, 1025
 Humphreys, R. M., Davidson, K., & Smith, N. 1999, PASP, 111, 1124
 Humphreys, R. M., Davidson, K., & Smith, N. 2002, AJ, 124, 1026
 Humphreys, R. M., Smith, N., Davidson, K., Jones, T. J., Gehrz, R. D., Mason, C. G., Hayward, T. L., Houck, J. R., & Krautter, J. 1997, AJ, 114, 2778
 Jura, M. 1991, Astron. & Astroph. Rev., 2, 227
 Kulkarni, S., et al. 2007, Nature, 447, 458
 Lejeune, T., & Schaerer, D. 2001, A&A, 366, 538
 Leonard, D. C., Gal-Yam, A., Fox, D. B., Cameron, P. B., Johansson, E. M., Kraus, A. L., Mignant, D. L., & van Dam, M. A. 2008, PASP, 120, 1259
 Li, W., Smith, N., Miller, A. A., & Filippenko, A. V. 2009, ATel, 2212, 1
 Li, W., Filippenko, A.V., Chornock, R., & Jha, S. 2003, ApJ, 586, L9
 Li, W., et al. 2007, ApJ, 661, 1013
 Maza, J., et al. 2009, CBET, 1928, 1
 Miller, A., Li, W., Nugent, P., Bloom, J. S., Filippenko, A. V., & Merritt, A. T. 2009, ATel, 2183, 1
 Mitchell, R. M., & Robinson, G. 1978, ApJ, 220, 841
 Nomoto, K. 1984, ApJ, 277, 791
 Nugent, P. E. 2009, BAAS, 41, 419.
 Oke, J. B., et al. 1995, PASP, 107, 375
 Osterbrock 1989, *Astrophysics of Gaseous Nebulae and Active Galactic Nuclei* (Mill Valley: University Science)
 Owocki, S. P., Gayley, K. G., & Shaviv, N. J. 2004, ApJ, 616, 525
 Pastorello, A., et al. 2007, Nature, 449, 1
 Petit, V., Drissen, L., & Crowther, P. A. 2006, AJ, 132, 1756
 Prieto, J. 2008, ATel, 1550, 1
 Prieto, J., et al. 2008, ApJ, 681, L9
 Prieto, J., et al. 2009, ApJ, 705, 1425
 Smith, N. 2004, MNRAS, 349, L31
 Smith, N. 2006, ApJ, 644, 1151
 Smith, N. 2007, AJ, 133, 1034
 Smith, N. 2008, Nature, 455, 201
 Smith, N. 2010, MNRAS, in press (arXiv:0910.4395)
 Smith, N., Humphreys, R. M., & Gehrz, R. D. 2001, PASP, 113, 692
 Smith, N., & Owocki, S. P. 2006, ApJ, 645, L45
 Smith, N., Vink, J., & de Koter, A. 2004, ApJ, 615, 475
 Smith, N., et al. 2003, AJ, 125, 1458
 Smith, N., et al. 2009, ApJ, 697, L49
 Smith, N., et al. 2010, ApJ, 709, 856
 Skrutskie, M., et al. 2006, AJ, 131, 1163
 Stahl, O. 1986, A&A, 164, 321
 Stahl, O. 1987, A&A, 182, 229
 Stahl, O. 1989, in *Physics of Luminous Blue Variables (Astrophysics & Space Science Library, Vol. 157)*, ed. K. Davidson, A. F. J. Moffat, & H. J. G. L. M. Lamers (Berlin: Springer), 149
 Stahl, O., & Wolf, B. 1986, A&A, 158, 371
 Stahl, O., et al. 1993, A&AS, 99, 167
 Szeifert, T., et al. 1996, A&A, 314, 131
 Tammann, G. A., & Sandage, A. 1968, ApJ, 151, 825
 Thompson, T. A., Prieto, J. L., Stanek, K. Z., Kistler, M. D., Beacom, J. F., & Kochanek, C. S. 2009, ApJ, 705, 1364
 Valeev, A.F., Sholukhova, O., & Fabrika, S. 2009, MNRAS, 396, L21
 Van Dyk, S. D., Filippenko, A. V., & Li, W. 2002, PASP, 114, 700
 Van Dyk, S. D., et al. 2005, PASP, 117, 553
 van Genderen, A. M. 2001, A&A, 366, 508
 Vogt, S. S., et al. 1994, Proc. SPIE, 2198, 362
 Walborn, N. R., Stahl, O., Gamen, R. C., Szeifert, T., Morrell, N. I., Smith, N., Howarth, I. D., Humphreys, R. M., Bond, H. E., & Lennon, D. J. 2008, ApJ, 683, L33
 Wesson, R., et al. 2010, MNRAS, in press (arXiv:0907.0246)
 Wizinowich, P., et al. 2006, PASP, 118, 297

Wolf, B. 1989, A&A, 217, 87
Wolf, B., & Stahl, O. 1990, A&A, 235, 340

Wolf, B., Stahl, O., Smolinski, J., & Casatella, A. 1988, A&AS, 74, 239